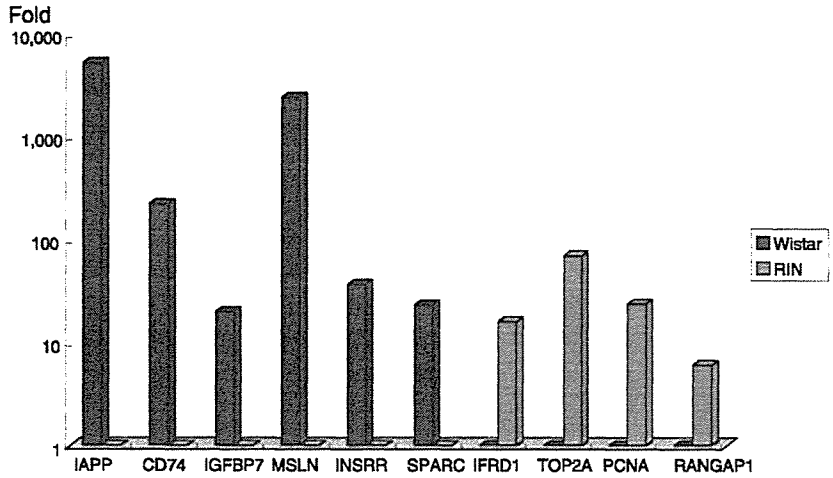

Figure 1 Expression profiles of the representative genes abundant either in islet (from Wistar rats) or in RINm5F cells. The expression levels of the genes were estimated by real-time quantitative RT-PCR using the TaqMan system. The mRNA for major α-globin could not be efficiently detected by the TaqMan system in its standard range for unknown reasons.

correlated with the Northern blot analysis, except for the low-frequency ESTs. Thus, the genes of interest that are expressed at least at moderate levels also should be examined by semi-quantitative analysis before further analysis.

We focus on the seven genes exhibiting high expression (>15 times) in islet but no expression in RINm5F cells (Table 5), since they may well play a specific role in insulin synthesis and secretion. Expression of all of the genes examined was confirmed in pancreatic β cells by *in situ* hybridization, although the expression was not restricted to β cells (Fig. 2A). The expression of the high EST clones (>15 times) in RINm5F cells and none in islets was found only outside the islets by *in situ* hybridization (Fig. 2B). These patterns of expression are consistent with a previous assumption that over 90% of the genes are house-keeping and are expressed at various levels in many tissues. Receptors of the insulin/insulin-like growth factor (IGF) family have been implicated both in the regulation of pancreatic β-cell growth and insulin secretion. IRR, an orphan receptor of the insulin receptor subfamily, is expressed at a considerably higher level in pancreatic β cells (Hirayama *et al.* 1999), and a decrease in the mRNA level was found in diabetic GK rats (N Shihara, Y Horikawa, J Takeda, unpublished observations). However, since glucose-stimulated insulin secretion and embryonic β cell development have been shown to occur normally in mice lacking IRR (Kitamura *et al.* 2001), decreased expression of IRR alone may be insufficient for the development of diabetes. To understand the functional properties of IRR in pancreatic β cells, it is important to identify its possible ligand and functional partners. Mesothelin, produced by mesothelial cells, has been suggested to play a role in cellular adhesion in ovarian cancer cells (Scholler *et al.* 1999). Since this EST was not found in cultured RINm5F cells, methothelin may well be unimportant in single-cell growth without cell adhesion and not directly involved in endocrine

Table 5 Genes abundantly identified either in islet or in RINm5F cells

Gene	Islet	RINm5F
Islet amyloid polypeptide (amylin)	321	0
CD74	28	0
Follistatin-like protein (mac25)	24	0
Mesothelin	23	0
Major alpha-globin	23	0
Insulin receptor-related receptor (IRR)	18	0
Osteonectin	17	0
Interferon-related developmental regulator 1	0	53
DNA topoisomerase II alpha	0	43
Proliferating cell nuclear antigen	0	26
Glycosyl-phosphatidyl-inositol-anchored protein homolog	0	24
Casein kinase 1 gamma 2 isoform	0	22
Ran-GTPase activating protein 1	0	21
Heat shock 70kD protein 5	0	20
High mobility group protein 17	0	17
Phosphoglycerate mutase type B subunit	0	17
Synaptic regulatory protein RIM2beta	0	17
Heat shock protein 60	0	17
HLA-B associated transcript 2	0	16
Secretory carrier membrane protein 3	0	15

Genes with high (>15 times) expression in either islet and RINm5F and none of the other, are listed.

tumorigenesis. CD74, which is transitorily associated with class II histocompatibility antigens during intracellular transport (Claesson *et al.* 1983), also was found to be highly expressed in human islet tumor in our previous study (Jin *et al.* 2003). Since this islet tumor exhibited features of moderately differentiated islet cells, despite markedly reduced insulin secretion, in contrast to RINm5F cells, CD74 might be related to the degree of cell differentiation. Osteonectin is reported to be abundantly expressed in adipose tissue. Although the molecule has not been reported to be expressed in islets, *in situ* hybridization showed that its expression is moderate in islet cells and diffuse throughout the pancreas of normal Wistar rat. It has been reported that absence of osteonectin leads to an increase in the size of individual adipocytes as well as in the number of adipocytes per fat pad (Bradshaw *et al.* 2003). Thus, osteonectin might be related to β cell mass and growth rather than insulin synthesis and secretion. As these genes might contribute to the development of islet cell specificity, their functional significance should be examined in various conditions of pancreatic islets.

Applications of rat ESTs for islet studies

In this study, we describe a collection of 40 710 rat pancreatic islet-related ESTs representing 10 406 different transcripts. This is the first report describing a systematic collection of rat expressed genes from pancreatic islets and a β-cell line. Since DNA microarray technology relies largely on the rapid growth of the EST databases, these newly identified expressed genes should facilitate analysis of differential gene expression in pancreatic islets under various conditions. At present, only the PanChip microarray, which was prepared using 3400 cDNA sequences from mouse whole pancreas, is available as a tissue-specific microarray for islet studies (Scearce *et al.* 2002). Accordingly, the establishment of islet-specific DNA microarrays for the rat should be especially important in the analysis of the transcriptome of diabetic rats such as GK and OLETF, and is presently underway in our laboratory. Another advantage of the large-scale collection of EST clones is that the cDNA fragments obtained can be used as hybridizing probes for Northern blotting or *in situ* hybridization to analyze the size and number of alternatively spliced transcripts and their local tissue distribution. However, it is possible that a small fraction of the ESTs obtained might be contaminated from other cell types such as endothelial cells or blood. Indeed, our preliminary trial of non-isotopic *in situ* hybridization using rat ESTs was found to be quite effective for analysis of mRNA expression in pancreatic islets. A large-scale *in situ* hybridization of rat islet mRNAs is also presently in progress in our laboratory. Functional analysis of a wide spectrum of islet-specific genes and genes highly abundant or less abundant in islets identified by this approach might clarify the molecular mechanisms underlying the differentiation of islet cells, tumorigenesis, and the pathogenesis of diabetes, as well as lead to new therapies for the improvement and regeneration of β-cell function through manipulation of gene expression and gene products.

In addition, as the genome sequence analysis of the Brown Norway rat recently has been completed (Rat Genome Sequencing Project Consortium 2004), the results of this study should be helpful in annotating the genes actually expressed in the rat genome and thus provide further insight into mammalian evolution of genes involved in tissue-specificity of endocrine pancreas.

Acknowledgements

We thank S Oike, R Kawakami, Y Yaginuma, I Uda, Y Ibe, and T Takahashi for excellent assistance. This study was supported by Grant-in-Aid for Scientific Research and for Scientific Research on Priority Areas (C) "Medical Genome Science" from the Japanese Ministry of Science, Education, Sports, Culture and Technology and by a Health and Labor Science Research Grant for Research on Human Genome and Tissue Engineering from the Japanese Ministry of Health, Labor and Welfare, the Naito Foundation and the Yamanouchi Foundation. The authors declare that there is no conflict of interest that would prejudice the impartiality of this scientific work.

References

Alberts B, Bray D, Lewis J, Raff M, Roberts K & Watson JD 1994 The cell nucleus. In: *Molecular Biology of the Cell*. pp 335–400. New York: Garland.

Altschul SF, Madden TL, Schaffer AA, Zhang J, Zhang Z, Miller W & Lipman DJ 1997 Gapped BLAST and PSI-BLAST: a new generation of protein database search programs. *Nucleic Acids Research* **25** 3389–3402.

Bernal-Mizrachi E, Cras-Meneur C, Ohsugi M & Permutt MA 2003 Gene expression profiling in islet biology and diabetes research. *Diabetes Metabolism Research Review* **19** 32–42.

Bonner-Weir S & Sharma A 2002 Pancreatic stem cells. *Journal of Pathology* **197** 519–526.

Bradshaw AD, Graves DC, Motamed K & Sage EH 2003 SPARC-null mice exhibit increased adiposity without significant differences in overall body weight. *PNAS* **100** 6045–6050.

Claesson L, Larhammar D, Rask L & Peterson PA 1983 cDNA clone for the human invariant gamma chain of class II histocompatibility antigens and its implications for the protein structure. *PNAS* **80** 7395–7399.

Dor Y, Brown J, Martinez OI & Melton DA 2004 Adult pancreatic β-cells are formed by self-duplication rather than stem-cell differentiation. *Nature* **429** 41–46.

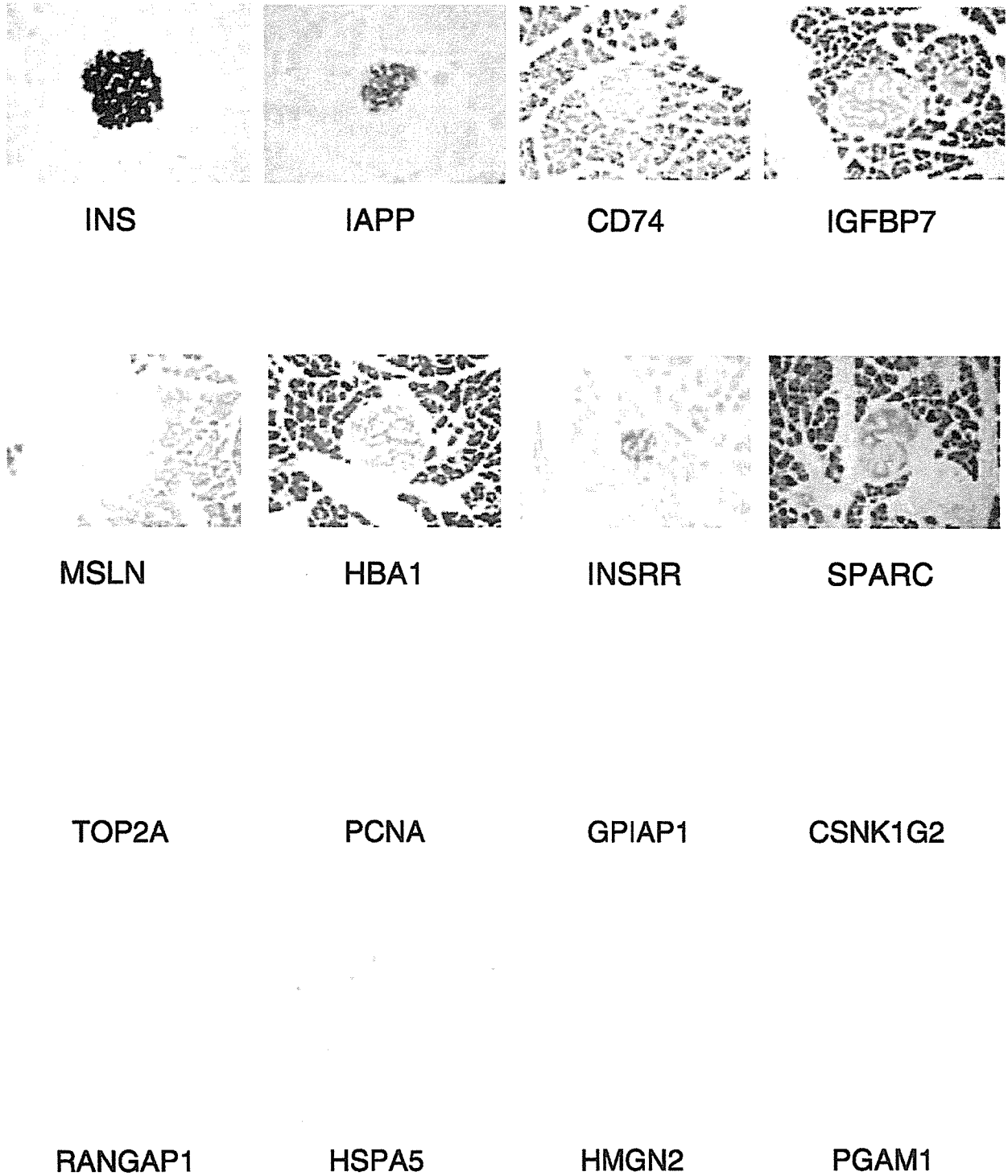

Figure 2 (A) *In situ* hybridization of genes with high expression in islet and none in RINm5F cells (A). The representative results of seven highly expressed genes (>15 times) and the insulin gene are shown. (B) *In situ* hybridization of genes with high expression in RINm5F cells and none in islet.

Edlund H 2002 Pancreatic organogenesis – Developmental mechanisms and implications for therapy. *Nature Genetics Review* **3** 524–532.

Fajans SS, Bell GI & Polonsky KS 2001 Molecular mechanisms and clinical pathophysiology of maturity-onset diabetes of the young. *New England Journal of Medicine* **345** 971–980.

Gazdar AF, Chick WL, Oie HK, Sims HL, King DL, Weir GC & Lauris V 1980 Continuous, clonal, insulin- and somatostatin-secreting cell lines established from a transplantable rat islet cell tumor. *PNAS* **77** 3519–3523.

Hirayama I, Tamemoto H, Yokota H, Kubo SK, Wang J, Kuwano H, Nagamachi Y, Takeuchi T & Izumi T 1999 Insulin receptor-related receptor is expressed in pancreatic beta-cells and stimulates tyrosine phosphorylation of insulin receptor substrate-1 and -2. *Diabetes* **48** 1237–1244.

Hogenesch JB, Ching KA, Batalov S, Su AI, Walker JR, Zhou Y, Kay SA, Schultz PG & Cooke MP 2001 A comparison of the Celera and Ensembl predicted gene sets reveals little overlap in novel genes. *Cell* **106** 413–415.

International Human Genome Sequencing Consortium 2001 Initial sequencing and analysis of the human genome. *Nature* **409** 860–921.

Jin L, Wang H, Narita T, Kikuno R, Ohara O, Shihara N, Nishigori T, Horikawa Y & Takeda J 2003 Expression profile of mRNAs from human pancreatic islet tumors. *Journal of Molecular Endocrinology* **31** 519–528.

Kayo T, Sawada Y, Suda M, Konda Y, Izumi T, Tanaka S, Shibata H & Takeuchi T 1997 Proprotein-processing endoprotease furin controls growth of pancreatic β-cells. *Diabetes* **46** 1296–1304.

Kitamura T, Kido Y, Nef S, Merenmies J, Parada LF & Accili D 2001 Preserved pancreatic β-cell development and function in mice lacking the insulin receptor-related receptor. *Molecular and Cellular Biology* **21** 5624–5630.

Lee NH, Weinstock KG, kirkness EF, Earle-Hughes JA, Fuldner RA, Marmaros S, Glodek A, Gocayne JD, Adams MD, Kerlavage AR, Fraser CM & Venter JC 1995 Comparative expressed-sequence-tag analysis of differential gene expression profiles in PC-12 cells before and after nerve growth factor treatment. *PNAS* **92** 8303–8307.

Ma H-T, Kato M & Tatemoto K 1996 Effects of pancreastatin and somatostatin on secretagogues-induced rise in intracellular free calcium in single rat pancreatic islet cells. *Regulatory Peptide* **61** 143–148.

Mouse Genome Sequencing Consortium 2002 Initial sequencing and comparative analysis of the mouse genome. *Nature* **420** 520–562.

Philippe J, Chick WL & Habener JF 1987 Multipotential phenotypic expression of genes encoding peptide hormones in rat insulinoma cell lines. *Journal of Clinical Investigation* **79** 351–358.

Rat Genome Sequencing Project Consortium 2004 Genome sequence of the Brown Norway rat yields insights into mammalian evolution. *Nature* **428** 493–521.

Scearce LM, Brestelli JE, McWeeney SK, Lee CS, Mazzarelli J, Pinney DF, Pizarro A, Stoeckert CJ Jr, Clifton SW, Permutt MA, Brown J, Melton DA & Kaestner KH 2002 Functional genomics of the endocrine pancreas: The pancreas clone set and PanChip, new resources for diabetes research. *Diabetes* **51** 1997–2004

Scholler N, Fu N, Yang Y, Ye Z, Goodman GE, Hellstrom KE & Hellstrom I 1999 Soluble member(s) of the mesothelin/megakaryocyte potentiating factor family are detectable in sera from patients with ovarian carcinoma. *PNAS* **96** 11531–11536.

Takeda J, Yano H, Eng S & Bell GI 1993 A molecular inventory of human pancreatic islets: sequence analysis of 1000 cDNA clones. *Human Molecular Genetics* **2** 1793–1798.

Venter JC, Adams MD, Myers EW, Li PW, Mural RJ, Sutton GG, Smith HO, Yandell M, Evans CA, Holt RA, *et al.* 2001 The sequence of the human genome. *Science* **291** 1304–1351.

Received 17 March 2005
Accepted 29 April 2005
Made available online as an Accepted Preprint 16 May 2005

0021-972X/05/$15.00/0
Printed in U.S.A.

The Journal of Clinical Endocrinology & Metabolism 90(10):5841–5847

doi: 10.1210/jc.2005-0991

Genetic Variation in the Hypoxia-Inducible Factor-1α Gene Is Associated with Type 2 Diabetes in Japanese

Norihiro Yamada, Yukio Horikawa, Naohisa Oda, Katsumi Iizuka, Nobuyuki Shihara, Shoji Kishi, and Jun Takeda

Department of Ophthalmology (N.Y., S.K.), Gunma University Graduate School of Medicine, 371-8511 Gunma, Japan; Laboratory of Medical Genomics, Biosignal Genome Resource Center (Y.H., N.S., J.T.), Institute for Molecular and Cellular Regulation, Gunma University, 371-8512 Gunma, Japan; Core Research for Evolutional Science and Technology (Y.H., K.I., N.S., J.T.), Japan Science and Technology Corporation, 332-0012 Kawaguchi, Japan; Department of Diabetes and Endocrinology (Y.H., J.T.), Gifu University School of Medicine, Gifu 501-1194, Japan; and Department of Internal Medicine (N.O.), Fujita Health University School of Medicine, 470-1192 Aichi, Japan

Context and Objective: Vascular endothelial growth factor plays a critical role both in neovascularization of proliferative diabetic retinopathy and in angiogenesis of islets in the pancreatic developmental stage in determining β-cell mass and properties. Vascular endothelial growth factor mRNA levels increase as a result of increased transcriptional activation, mediated predominantly by hypoxia-inducible factor-1 α (HIF-1α) in response to hypoxia.

Design and Patients: In this study, we examined all regions of the HIF-1α to detect single-nucleotide polymorphisms (SNPs), evaluated the pattern of linkage disequilibrium to analyze haplotypes, and performed association studies in Japanese type 2 diabetes patients with or without retinopathy.

Results: A total of 35 SNPs were found in the gene, 27 of which were reported previously and eight of which were novel. Three of the 35 SNPs were located in coding regions, one in exon 2 (S28Y), and the others in exon 12 (P582S, A588T). The P582S HIF-1α mutation was associated with type 2 diabetes ($P = 0.0028$) by a consistently higher level of transcriptional activity than wild type, especially under hypoxic condition ($P = 0.012$), but no association with retinopathy was detected.

Conclusion: This is the first report that HIF-1α is associated with the occurrence of type 2 diabetes and suggests that the P582S HIF-1α mutation should be assessed in larger studies as a risk factor for type 2 diabetes. (***J Clin Endocrinol Metab* 90: 5841–5847, 2005**)

DIABETES LEADS TO specific microvascular complications of retinopathy, nephropathy, and neuropathy as well as increased risk of atherosclerosis, which may reflect underlying endothelial dysfunction. The risk of developing these complications is increased by poor glycemic control, but the relevance of genetic background is clearly established (1–3).

Diabetic retinopathy is a major cause of new-onset blindness among diabetic adults and is characterized by increased vascular permeability, tissue ischemia, and neovascularization. Neovascularization of the retina carries a high risk of blindness as a result of vitreous hemorrhage, fibrosis, and tractional retinal detachment. Vascular endothelial growth factor (VEGF) can stimulate angiogenesis, enhance collateral vessel formation, and increase permeability of the microvasculature (4). In diabetic proliferative retinopathy, VEGF plays a critical role in neovascularization and breakdown of the blood-retinal barrier characterized by hyperpermeability of retinal vessels. VEGF levels have been found to be markedly elevated in vitreous and aqueous fluids in the eyes of patients with proliferative diabetic retinopathy (PDR) (5). Furthermore, VEGF has been reported as a susceptibility gene for type 2 diabetes mellitus (T2DM) as well as diabetic retinopathy (6). VEGF is known to be a key factor in angiogenesis of islets in the pancreatic developmental stage in determining β-cell mass and properties (7). In response to hypoxia, VEGF mRNA levels are increased by increased transcriptional activation, whereas overall protein synthesis is inhibited. This increase is mediated predominantly by hypoxia-inducible factor-1 (HIF-1) binding to a hypoxia response element located 1 kb upstream of the transcriptional start site of VEGF (8, 9).

HIF-1, a transcription factor found in mammalian cells cultured under reduced oxygen tension, plays an essential role in cellular and systemic homeostatic responses to hypoxia. HIF-1 acts as a heterodimer composed of a 120-kDa HIF-1α subunit complexed with a 91- to 94-kDa HIF-1β subunit (10). Although HIF-1β is ubiquitously expressed and maintained at constant cellular levels, the HIF-1α protein level and transcriptional activity are tightly regulated in response to oxygen levels. Thus, HIF-1 activity is controlled by the oxygen-regulated expression of the HIF-1α subunit (11). Under nonhypoxic conditions, HIF-1α is hydroxylated on proline residues by a family of oxygen-dependent prolyl hydroxylases. The hydroxylated prolines independently mediate high-affinity binding to the von Hippel-Lindau (VHL) protein, a component of the E3 ubiquitin-protein ligase com-

First Published Online July 26, 2005

Abbreviations: BMI, Body mass index; CI, confidence interval; cSNP, coding SNP; HbA_{1c}, glycosylated hemoglobin; HDL, high-density lipoprotein; HIF-1α, hypoxia-inducible factor-1α; HT, hypertension; LD, linkage disequilibrium; OR, odds ratio; PDR, proliferative diabetic retinopathy; SNP, single-nucleotide polymorphism; T-chol, total cholesterol; T2DM, type 2 diabetes mellitus; TG, triglyceride; TK, thymidine kinase; VEGF, vascular endothelial growth factor; VHL, von Hippel-Lindau.

JCEM is published monthly by The Endocrine Society (http://www.endo-society.org), the foremost professional society serving the endocrine community.

plex that ubiquitinates HIF-1α, thereby targeting it for degradation. The critical proline residues for VHL binding when hydroxylated are P402 and P564, both of which are located in the oxygen-dependent degradation domain (12, 13)

The HIF-1α gene is located at chromosome 14q21-q24, where the susceptibility locus to T2DM was localized in Finns (14). The predicted 826-amino-acid HIF-1α contains a basic helix-loop-helix-Per-Arnt-Sim (PAS) domain at its N terminus and a transactivation domain and transcriptional inhibitory domain at its C terminus (15). HIF-1 target genes include those for energy metabolism, iron homeostasis, angiogenesis, and cell proliferation and viability (16). Thus, HIF-1α activates many genes in the glycolysis system under conditions of hypoxia differently from insulin (17). In addition, the involvement of HIF-1 in the pathophysiology of human disease including myocardial ischemia, cerebral ischemia, retinal ischemia, pulmonary hypertension, preeclampsia, intrauterine growth retardation, and cancer has been reported (16). However, the correlations between HIF-1 and T2DM including complications remain to be elucidated.

In this study, we examined all regions of the HIF-1α gene in Japanese subjects to detect single-nucleotide polymorphisms (SNPs), evaluated the pattern of linkage disequilibrium (LD) to compose haplotypes in the gene, and performed association studies in T2DM patients. We identified a susceptibility coding SNP (cSNP) (P582S) and haplotype in the HIF-1α gene for T2DM. This is the first report suggesting that HIF-1α is associated with the occurrence of T2DM.

Subjects and Methods

Subjects

A total of 440 patients with T2DM [245 males and 195 females; age at testing, 60.5 ± 11.4 yr; duration, 11.4 ± 9.1 yr; body mass index (BMI), 23.9 ± 4.3 kg/m^2; maximum BMI, 27.5 ± 4.6 kg/m^2; glycosylated hemoglobin (HbA_{1c}), 7.9 ± 3.8%; total cholesterol (T-chol), 0.52 ± 0.11 mmol/liter; high-density lipoprotein (HDL), 0.13 ± 0.04 mmol/liter; triglyceride (TG), 0.39 ± 0.25 mmol/liter) and 572 controls (231 males and 342 females; age at testing, 67.3 ± 6.5 yr; BMI, 23.0 ± 2.9 kg/m^2; HbA_{1c}, 5.0 ± 0.4%) were examined for an association study. The diagnosis of T2DM was based on medical records or 75-g oral glucose tolerance test according to the criteria of the Japan Diabetes Society (18). One hundred eighty-two T2DM patients with retinopathy [80 males and 102 females; PDR, n = 117; pre-PDR, n = 29; and simple diabetic retinopathy, n = 36; age at testing, 61.9 ± 11.2 yr; duration, 13.0 ± 9.7 yr; BMI, 23.7 ± 3.9 kg/m^2; maximum BMI, 27.9 ± 6.6 kg/m^2; HbA_{1c}, 7.6 ± 1.9%; T-chol, 0.52 ± 0.14 mmol/liter; HDL, 0.12 ± 0.04 mmol/liter; TG, 0.41 ± 0.20 mmol/liter; hypertension (HT) drug use, 94 (−)/88(+); insulin therapy, 105(−)/77(+)] and 125 without retinopathy (47 males and 78 females; age at testing, 62.9 ± 11.6 yr; duration, 11.0 ± 8.6 yr; BMI, 23.7 ± 4.8 kg/m^2; maximum BMI, 26.1 ± 6.6 kg/m^2; HbA_{1c}, 6.8 ± 1.4%; T-chol, 0.50 ± 0.10 mmol/liter; HDL, 0.10 ± 0.04 mmol/liter; TG, 0.36 ± 0.22 mmol/liter; HT drug use, 99(−)/26(+); insulin therapy, 89(−)/36(+)]were examined by an association study with special reference to retinopathy. An additional 88 patients diagnosed with PDR by an ophthalmologist were included in the patients with retinopathy. Control subjects were recruited on the following criteria: 60 or more years of age, no past history of diagnosis of diabetes mellitus, HbA_{1c} less than 5.6%, and no familial history of diabetes mellitus in second-degree relatives. The study was approved by the Ethics Committee of Gunma University and Fujita Health University School of Medicine upon written, informed consent of each subject.

SNP identification in the HIF-1α gene

Genomic DNA was extracted from samples of whole blood using QIAamp DNA blood kit (QIAGEN, Hilden, Germany) according to the manufacturer's instructions. Sixteen of the random control samples (32 alleles) were used to detect SNPs in the HIF-1α gene. Primers for PCR experiments were designed by Primer 3 (available from http://www.genome.wi.mit.edu/cgi-bin/primer/primer3_www.cgi) on the basis of the genomic contig sequence (GenBank accession number NT_026437) of the HIF-1α region. The mixture for PCR was 20 μl in 10 ng template DNA, 0.5 mM of each dNTP, 2.5 pmol of each forward and reverse primer, 0.5 U Ex*Taq* polymerase (Takara, Kyoto, Japan), and 2 μl of 10× PCR buffer. The reaction conditions were an initial denaturation step of 95 C for 3 min and a subsequent 40 cycles of reaction at 94 C for 30 sec, 52–63 C for 30 sec, and 72 C for 1 min, and a final extension step of 72 C for 10 min. A 3-μl aliquot from each reaction was assayed on a 1% agarose gel to confirm the product, and the remainder was purified using MultiScreen Filtration System (Millipore, Billerica, MA) with Sephadex G-75 (Amersham Biosciences, Piscataway, NJ). Each PCR product was subjected to cycle sequencing with BigDye Terminator cycle sequencing FS (Applied Biosystems, Foster City, CA) using each forward and reverse primer. Reaction products were purified by ethanol precipitation and sequenced by ABI PRISM 3100 or 3700 sequencer. Results were processed with Autoassembler version 2.1 (Applied Biosystems) to compare sequences.

Mutation screening and genotyping of frequent polymorphisms in the HIF-1α gene

We examined all of the coding regions of the HIF-1α gene in 96 of the 440 T2DM patients (59 males and 37 females; age, 58.6 ± 12.1 yr; age at diagnosis, 44.2 ± 12.7 yr; duration, 14.4 ± 9.2 yr; BMI, 23.7 ± 3.8 kg/m^2; maximum BMI, 28.9 ± 4.5 kg/m^2; HbA_{1c}, 7.3 ± 1.5%) and 96 of the 576 control subjects (35 males and 61 females; age, 67.6 ± 5.8 yr; BMI, 22.9 ± 2.8 kg/m^2; HbA_{1c}, 4.9 ± 0.3%). Twenty-four frequent SNPs were examined in the 440 T2DM patients and 572 controls by direct sequencing or TaqMan assay (Applied Biosystems). PCR was performed in a total volume of 5 μl, which contained 2.5 ng DNA, 1× TaqMan Universal PCR Master Mix, with each primer at a concentration of 900 nM and each probe at a concentration of 200 nM. Thermal cycling conditions were as follows: 50 C for 2 min and 95 C for 10 min to activate the amperase uracil-*N*-glycosylase and AmpliTaq Gold enzyme, respectively, followed by 40 cycles of 92 C for 15 sec and 52–63 C for 1 min. The fluorescence level was measured with an ABI PRISM 7900HT sequence detector (Applied Biosystems), resulting in clear identification of three genotypes.

Estimation of haplotype frequencies and evaluation of pattern of LD in the HIF-1α gene

Haplotypes and haplogenotypes were inferred by the expectation-maximization method by Haploview (http://www.broad.mit.edu/personal/jcbarret/haploview) and PHASE 2.1.1 (http://www.stat.washington.edu/stephens), respectively. The coefficients for LD, D', and r^2 value were estimated by GOLD software (available from http://www.well.ox.ac.uk/asthma/GOLD).

Cloning of human HIF-1α and variants

A cDNA identical to HIF-1α was retrieved from a human islet cDNA library and subcloned in pENTR/D-TOPO (Invitrogen, Carlsbad, CA) after amplification with Pfu (Stratagene, La Jolla, CA) and the primer set 5′-CACCATGGAGGGCGCCGGCGGCGCGAAC-3′ and 5′-TCAGTTAACTTGATCCAAAGCTCTG-3′ and transferred for expression to pcDNA3.2-DEST (Invitrogen). The P582S mutation was introduced by QuikChange site-directed mutagenesis kit (Stratagene) with pENTR/D-TOPO wild-type HIF-1α as template and confirmed by sequencing.

Functional analysis of the identified HIF-1α mutation

The reporter construct VEGF promoter-pGL3 was prepared by cloning the human VEGF gene promoter (−1180 to ~+338) into the firefly luciferase reporter vector pGL3-Basic (Promega, Madison, WI) (17). HEK293 cells were maintained in DMEM supplemented with 10% fetal calf serum and transfected using ExGen 500 (Fermentas, St. Leon-Rot, Germany) with various amounts of the reporter and test plasmid constructs. Transcriptional activity was normalized with a cotransfected control thymidine kinase (TK)-regulated Renilla luciferase vector,

pRL-TK (Promega). The transactivation activity of wild-type and mutant proteins was measured using the Dual-Luciferase Reporter Assay System (Promega). After 6 h transfection, the cells were incubated 24 h under normoxic (21% O_2) or hypoxic (1% O_2) conditions using Anaero Pack (Mitsubishi Gas Chemical, Tokyo, Japan) before analysis of reporter gene activity.

Statistical analyses

Statistical difference in allele frequencies between T2DM and control groups or between T2DM with and without retinopathy groups was assessed by χ^2 test, and other categorical clinical variables were compared using t test or logistic regression analysis adjusted for relevant covariates. Statistical analysis was performed with StatView 5.0 software (SAS Institute, Inc., Cary, NC).

Results

Identification of polymorphisms in the HIF-1α gene

Sixteen individuals were examined for sequence variations in 38 kb of the 78-kb region of the HIF-1α gene including all 15 exons (NT_026437, nucleotides 61222006–61300408). A total of 35 SNPs were found in the gene; the locations of these SNPs are shown in Fig. 1 in relation to the genomic structure of the HIF-1α gene. All SNPs were in Hardy-Weinberg equilibrium, and 27 were reported in the Institute of Medical Science-Japan Science and Technology Agency SNP database (http://snp.ims.u-tokyo.ac.jp/index.html) or in the National Center for Biotechnology Information SNP database (http://www.ncbi.nlm.nih.gov/SNP/). Eight SNPs (SNP-6, SNP-12, SNP-18, SNP-19, SNP-31, SNP-32, SNP-33, and SNP-34) were novel and had not been reported. Three of the 35 SNPs were located in coding regions, one in exon 2 (S28Y), and the other SNPs in exon 12 (P582S, A588T) (Table 1).

Evaluation of pattern of LD in the HIF-1α gene

Twenty-three SNPs were used to define haplotypes and evaluate the pattern of LD in the 440 T2DM patients and 572 control subjects. As shown in Fig. 2, one LD block appears in this region in both groups. The five SNPs at position SNP-22 (g.25200), SNP-23 (g.25299), SNP-24 (g.27009), SNP-26 (g.34942), SNP-27 (g.35074), and the three SNPs at position SNP-14 (g.45483), SNP-16 (g.46572), and SNP-17 (g.46820) are in complete LD.

Mutation screening and association study of genetic variation of the HIF-1α gene in T2DM patients

All exons were examined in 96 T2DM patients and 96 control subjects. We found a total of three cSNPs (S28Y, P582S, and A588T), of which S28Y is novel. We then performed an association study using possible pairwise haplotypes in T2DM patients and controls. Ten SNPs (SNP-30, -2, -3, -4, -25, -7, -18, -20, -13, and -28) were used to define haplotypes. The other SNPs were excluded because of the rarity of minor alleles. We found that a haplotype comprising SNP-25 and SNP-13, which are in strong LD, represents significant susceptibility to T2DM at a P value of 10^{-11} based on a two by four χ^2 test, and also after multiple adjustment. The 1-1/2-2 haplogenotype comprising these two SNPs was associated with significantly decreased risk of T2DM [T2DM, 25.5%; control, 32.0%; odds ratio (OR) = 0.73; 95% confidence interval (CI), 0.55–0.96; $1 - \beta = 53\%$). The 2-2/2-2 haplogenotype also was associated with decreased risk (T2DM, 2.8%; control, 5.1%; OR = 0.51; 95% CI, 0.27–1.08), but the difference was not significant because of the small sample. As shown in Table 2, the P582S mutant allele was found with significantly less frequency in T2DM patients than in control subjects ($P = 0.0028$; $1 - \beta = 52\%$) and also was significant after adjustment for sex, age, and BMI by logistic regression analysis ($P = 0.0048$). Interestingly, the P582S mutant allele is completely assigned on the 2-2 haplotype of SNP-25 and SNP-13, which was observed more frequently in control subjects with strong statistical significance (Fig. 3). Accordingly, the mutant allele S582 is a representative SNP of the 2-2 haplotype, which contributes to decreased risk of T2DM. Indeed, if a dominant model is assumed, the S582 HIF-1α mutation is associated with decreased risk of T2DM (OR = 0.57; 95% CI, 0.37–0.88; $P = 0.010$).

Similar haplotypes were also identified at significant levels in patients with and without retinopathy, but none reached statistical significance after multiple adjustment (data not shown). We also performed an association study using single polymorphisms in patients with and without retinopathy, resulting in identification of two significant SNPs (SNP-15 and -29 at P values of 0.033 and 0.045, respectively), although these were also not statistically significant after multiple adjustment and adjustment for sex, age, duration, HbA_{1c}, BMI, T-chol, TG, presence of medicine for HT, and presence of insulin therapy by logistic regression analysis (data not shown).

Hypoxia-dependent transactivation of polymorphic HIF-1α

The transcriptional activity of the S582 HIF-1α mutant was then compared with that of wild type under normoxic or hypoxic conditions. The HIF-1α vectors were transfected into HEK293 cells with a firefly luciferase reporter gene regulated by human VEGF gene promoter and with a control TK-regulated Renilla luciferase vector. The mutant S582 HIF-1α showed a hypoxia-dependent increase in transcription ac-

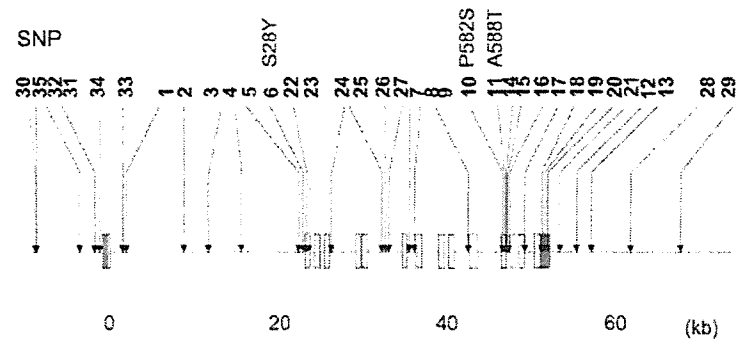

FIG. 1. Polymorphisms of *HIF1A* identified in this study. Nucleotide indicates the location of the SNP relative to the A of ATG of the initiator Met of *HIF1A* (GenBank no. NT_026437).

TABLE 1. Polymorphisms identified in *HIF1A* region in this study

SNP	Position genome	JSNP ID	dbSNP ID	Amino acid change	Variation	Location	Frequency of minor allele
30	−8393		rs7400961		C→G	5′ flanking	0.19
35	−8088		rs12717492		G→A	5′ flanking	0.19
32[a]	−7058				A→G	5′ flanking	0.06
31[a]	−4800				T→C	5′ flanking	0.09
34[a]	−1169				ACT/−	5′ flanking	0.01
33[a]	−907				T→C	5′ flanking	0.01
1	2506	IMS-JST057041	rs2301104		G→C	Intron 1	0.09
2	2598	IMS-JST057042	rs2301105		C→T	Intron 1	0.16
3	8904	IMS-JST023401	rs1951795		C→A	Intron 1	0.23
4	23170	IMS-JST140142	rs3783752		G→A	Intron 1	0.22
5	23956	IMS-JST035040	rs2284999		T→C	Intron 1	0.19
6[a]	24625			S28Y	C→A	Exon 2	0.01
22	25200		rs10137588		G→T	Intron 2	0.19
23	25299		rs10148514		T→C	Intron 2	0.19
24	27009		rs4899056		C→T	Intron 4	0.19
25	34776		rs12434438		A→G	Intron 6	0.25
26	34942	IMS-JST057045	rs2301108		G→A	Intron 6	0.19
27	35074	IMS-JST057046	rs2301109		A→G	Intron 6	0.19
7	37679	IMS-JST057048	rs2301111		C→G	Intron 7	0.22
8	37996	IMS-JST057049	rs966824		C→T	Intron 7	0.18
9	44026	IMS-JST057051	rs2301113		A→C	Intron 10	0.45
10	45035		rs11549465	P582S	C→T	Exon 12	0.06
11	45053		rs11549467	A588T	G→A	Exon 12	0.04
14	45483		rs4902080		C→T	Intron 12	0.21
15	45952		rs4902081		C→G	Intron 12	0.46
16	46572		rs8020184		T→C	Intron 12	0.20
17	46820	IMS-JST140141	rs3783751		G→C	Intron 12	0.21
18[a]	48445				G→T	Intron 14	0.23
19[a]	50292				C→T	3′ UTR	0.05
20	51326		rs2057482		C→T	3′ UTR	0.17
21	52853		rs994740		C→T	3′ UTR	0.16
12[a]	53485				C→G	3′ flanking	0.25
13	56703		rs1319462		A→G	3′ flanking	0.20
28	62194		rs7143626		G→A	3′ flanking	0.50
29	68040		rs2165601		T→C	3′ flanking	0.16

Nucleotide indicates the location of the SNP relative to the A of ATG of the initiator Met of *HIF1A* (GenBank no. NT_026437). Frequencies of minor alleles of SNPs in this table are observed in random control samples. JSNP, Japanese Single Nucleotide Polymorphism; dbsnp, SNPs deposited in the NCBI.

[a] Novel polymorphism.

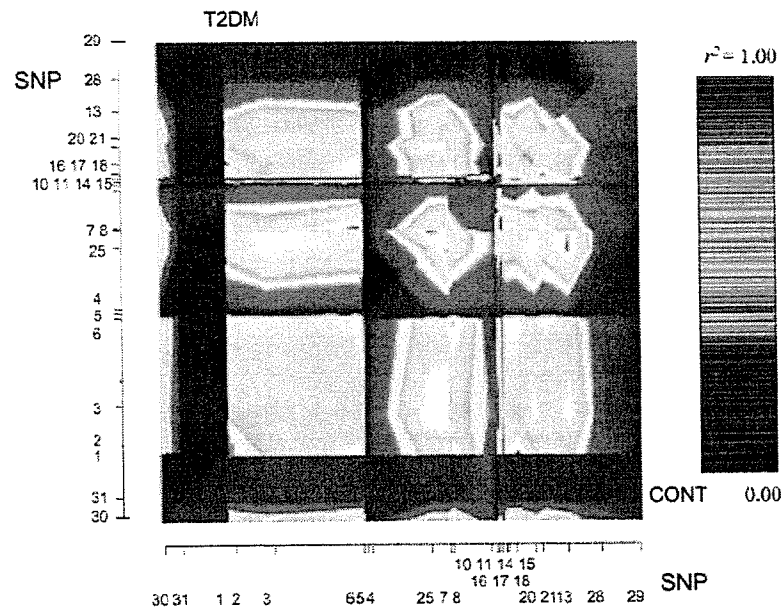

FIG. 2. Pairwise LD in *HIF1A* evaluated by r^2. Pairwise LD was determined using 276 marker pairs. Color gradations from *red* (perfect LD, *i.e.* $r^2 = 1$) to *blue* (no LD, *i.e.* $r^2 = 0$) reflect the degree of the observed LD. The *upper triangle* shows LD pattern estimated with 440 T2DM patients, and the *lower triangle* shows that with 576 controls (CONT).

age, BMI, HbA_{1C}, and the presence or absence of insulin therapy (data not shown), partly because of the small number of samples. Functional analysis of the mutant protein S582 HIF-1α using β-cell- or endothelium-derived cell lines might also be required. We did not detect a significant difference in P582S allele frequencies in patients with or without retinopathy, but additional studies with an increased number of patients classified with precise clinical information are required to assess the correlation of this variant with diabetic retinopathy.

It has been reported that acute intensive insulin therapy results in transcriptional activation of VEGF via p38 MAPK, phosphatidylinositol-3-kinase, and HIF-1α, producing paradoxical worsening of diabetic blood-retinal barrier breakdown (31). Thus, more attention should be paid to patients with the P582S HIF-1α mutant allele when they begin treatment with insulin therapy. This polymorphism should be further assessed in larger studies as a risk factor for the development of T2DM and as a biomarker for responses to specific therapies, antiangiogenic therapies in particular.

Acknowledgments

We thank S. Oike, R. Kawakami, Y. Yaginuma, I. Uda, Y. Ibe, and T. Takahashi for assistance.

Received May 5, 2005. Accepted July 18, 2005.

Address all correspondence and requests for reprints to: Yukio Horikawa, M.D., Ph.D., Department of Diabetes and Endocrinology, Gifu University School of Medicine, 1-1 Yanagido, Gifu-city, Gifu 501-1194, Japan. E-mail: yhorikaw@cc.gifu-u.ac.jp.

This study was supported by Grant-in-Aid for Scientific Research and for Scientific Research on Priority Areas (C) Medical Genome Science from the Japanese Ministry of Science, Education, Sports, Culture, and Technology; a Health and Labor Science Research Grant for Research on Human Genome and Tissue Engineering from the Japanese Ministry of Health, Labor, and Welfare; and the Naito Foundation.

References

1. 1997 Report of the Expert Committee on the Diagnosis and Classification of Diabetes Mellitus. Diabetes Care 20:1183–1197
2. **Diabetes Control and Complications Trial Research Group** 1997 Clustering of long-term complications in families with diabetes in the diabetes control and complications trial. Diabetes 46:1829–1839
3. **Rema M, Saravanan G, Deepa R, Mohan V** 2002 Familial clustering of diabetic retinopathy in South Indian type 2 diabetic patients. Diabet Med 19:910–916
4. **Duh E, Aiello LP** 1999 Vascular endothelial growth factor and diabetes: the agonist versus antagonist paradox. Diabetes 48:1899–1906
5. **Aiello LP, Avery RL, Arrigg PG, Keyt BA, Jampel HD, Shah ST, Pasquale LR, Thieme H, Iwamoto MA, Park JE, Nguyen HV, Aiello LM, Ferrara N, King GL** 1994 Vascular endothelial growth factor in ocular fluid of patients with diabetic retinopathy and other retinal disorders. N Engl J Med 331:1480–1487
6. **Awata T, Inoue K, Kurihara S, Ohkubo T, Watanabe M, Inukai K, Inoue I, Katayama S** 2002 A common polymorphism in the 5′-untranslated region of the VEGF gene is associated with diabetic retinopathy in type 2 diabetes. Diabetes 51:1635–1639
7. **Lammert E, Cleaver O, Melton D** 2001 Induction of pancreatic differentiation by signals from blood vessels. Science 294:564–567
8. **Forsythe JA, Jiang BH, Iyer NV, Agani F, Leung SW, Koos RD, Semenza GL** 1996 Activation of vascular endothelial growth factor gene transcription by hypoxia inducible factor 1. Mol Cell Biol 16:4604–4613
9. **Liu Y, Cox SR, Morita T, Kourembanas S** 1995 Hypoxia regulates vascular endothelial growth factor gene expression in endothelial cells. Circ Res 77:638–643
10. **Wang GL, Semenza GL** 1993 General involvement of hypoxia-inducible factor 1 in transcriptional response to hypoxia. Proc Natl Acad Sci USA 90:4304–4308
11. **Wang GL, Jiang BH, Rue EA, Semenza GL** 1995 Hypoxia-inducible factor 1 is a basic-helix-loop-helix-PAS heterodimer regulated by cellular O_2 tension. Proc Natl Acad Sci USA 92:5510–5514
12. **Maxwell PH, Wiesener MS, Chang GW, Clifford SC, Vaux EC, Cockman ME, Wykoff CC, Pugh CW, Maher ER, Ratcliffe PJ** 1999 The tumor suppressor protein VHL targets hypoxia-inducible factors for oxygen-dependent proteolysis. Nature 399:271–275
13. **Huang LE, Gu J, Schau M, Bunn HF** 1998 Regulation of hypoxia-inducible factor α is mediated by an O_2-dependent degradation domain via the ubiquitin-proteasome pathway. Proc Natl Acad Sci USA 95:7987–7992
14. **Silander K, Scott LJ, Valle TT, Mohlke KL, Stringham HM, Wiles KR, Duren WL, Doheny KF, Pugh EW, Chines P, Narisu N, White PP, Fingerlin TE, Jackson AU, Li C, Ghosh S, Magnuson VL, Colby K, Erdos MR, Hill JE, Hollstein P, Humphreys KM, Kasad RA, Lambert J, Lazaridis KN, Lin G, Morales-Mena A, Patzkowski K, Pfahl C, Porter R, Rha D, Segal L, Suh YD, Tovar J, Unni A, Welch C, Douglas JA, Epstein MP, Hauser ER, Hagopian W, Buchanan TA, Watanabe RM, Bergman RN, Tuomilehto J, Collins FS, Boehnke M; Finland-United States Investigation of NIDDM Genetics (FUSION)** 2004 A large set of Finnish affected sibling pair families with type 2 diabetes suggests susceptibility loci on chromosomes 6, 11, and 14. Diabetes 53:821–829
15. **Iyer NV, Leung SW, Semenza GL** 1998 The human hypoxia-inducible factor 1α gene: *HIF1A* structure and evolutionary conservation. Genomics 52:159–165
16. **Semenza GL** 2000 HIF-1 and human disease: one highly involved factor. Genes Dev 14:1983–1991
17. **Yim S, Choi SM, Choi Y, Lee N, Chung J, Park H** 2003 Insulin and hypoxia share common target genes but not the hypoxia-inducible factor-1α. J Biol Chem 278:38260–38268
18. **Kuzuya T, Nakagawa S, Satoh, J, Kanazawa Y, Iwamoto Y, Kobayashi M, Nanjo K, Sasaki A, Seino Y, Ito C, Shima K, Nonaka K, Kadowaki T** 2002 Report of the committee of the Japan Diabetes Society on the classification and diagnostic criteria of diabetes mellitus. Diabetes Res Clin Pract 55:65–85
19. **Horikawa Y, Oda N, Cox NJ, Li X, Orho-Melander M, Hara M, Hinokio Y, Lindner TH, Mashima H, Schwarz PE, del Bosque-Plata L, Horikawa Y, Oda Y, Yoshiuchi I, Colilla S, Polonsky KS, Wei S, Concannon P, Iwasaki N, Schulze J, Baier LJ, Bogardus C, Groop L, Boerwinkle E, Hanis CL, Bell GI** 2000 Genetic variation in the gene encoding calpain-10 is associated with type 2 diabetes mellitus. Nat Genet 26:163–175
20. **Altshuler D, Hirschhorn JN, Klannemark M, Lindgren CM, Vohl MC, Nemesh J, Lane CR, Schaffner SF, Bolk S, Brewer C, Tuomi T, Gaudet D, Hudson TJ, Daly M, Groop L, Lander ES** 2000 The common PPARγ Pro12Ala polymorphism is associated with decreased risk of type 2 diabetes. Nat Genet 26:76–80
21. **Ioannidis JP, Trikalinos TA, Ntzani EE, Contopoulos-Ioannidis DG** 2003 Genetic associations in large versus small studies: an empirical assessment. Lancet 361:567–571
22. **Frank RN** 2004 Diabetic retinopathy. N Engl J Med 350:48–58
23. **Yamada N, Shihara N, Horikawa Y, Wang H, Takeda J, Kishi S** 2005 Expression profile of 1000 mRNAs from rat retina. Kitakanto Med J 55:5–12
24. **Anastasiadis AG, Ghafar MA, Salomon L, Vacherot F, Benedit P, Chen MW, Shabsigh A, Burchardt M, Chopin DK, Shabsigh R, Buttyan R** 2002 Human hormone-refractory prostate cancers can harbor mutations in the O_2-dependent degradation domain of hypoxia inducible factor-1α (HIF-1α). J Cancer Res Clin Oncol 128:358–362
25. **Clifford SC, Astuti D, Hooper L, Maxwell PH, Ratcliffe PJ, Maher ER** 2001 The PVHL-associated SCF ubiquitin ligase complex: molecular genetic analysis of elongin B and C, Rbx 1 and HIF-1α in renal cell carcinoma. Oncogene 20:5067–5074
26. **Ollerenshaw M, Page T, Hammonds J, Demaine A** 2004 Polymorphisms in the hypoxia inducible factor-1α gene (*HIF1A*) are associated with the renal cell carcinoma phenotype. Cancer Genet Cytogenet 153:122–126
27. **Fu XS, Choi E, Bubley GJ, Balk SP** 2005 Identification of hypoxia-inducible factor-1α (HIF-1α) polymorphism as a mutation in prostate cancer that prevents normoxia-induced degradation. Prostate 63:215–221
28. **Tanimoto K, Yoshiga K, Eguchi H, Kaneyasu M, Ukon K, Kumazaki T, Oue N, Yasui W, Imai K, Nakachi K, Poellinger L, Nishiyama M** 2003 Hypoxia-inducible factor-1α polymorphisms associated with enhanced transactivation capacity, implying clinical significance. Carcinogenesis 24:1779–1783
29. **Percy MJ, Mooney SM, McMullin MF, Flores A, Lappin TR, Lee FS** 2003 A common polymorphism in the oxygen-dependent degradation (ODD) domain of hypoxia inducible factor-1α (HIF-1α) does not impair Pro-564 hydroxylation. Mol Cancer 2:31
30. **Moritz W, Meier F, Stroka DM, Giuliani M, Kugelmeier P, Nett PC, Lehmann R, Candinas D, Gassmann M, Weber M** 2002 Apoptosis in hypoxic human pancreatic islets correlates with HIF 1α expression. FASEB J 16:745–747
31. **Poulaki V, Qin W, Joussen AM, Hurlbut P, Wiegand SJ, Rudge J, Yancopoulos GD, Adamis AP** 2002 Acute intensive insulin therapy exacerbates diabetic blood-retinal barrier breakdown via hypoxia-inducible factor-1α and VEGF. J Clin Invest 109:805–815

SNP-25	SNP-7	SNP-8	SNP-9	SNP-10 (P582S)	SNP-14	SNP-15	SNP-18	SNP-20	SNP-12	SNP-13	Frequency CONT	Frequency T2DM
1	1	1	1	1	1	1	1	1	1	1	0.537	0.543
1	1	1	2	1	1	2	1	1	1	1	0.213	0.215
2	2	2	2	1	2	2	2	2	2	2	0.108	0.085
2	2	1	2	**2**	1	2	1	2	1	2	0.070	0.035
2	2	2	2	1	2	2	1	2	2	2	0.017	0.022
2	2	2	1	1	1	1	2	1	1	2	0.017	0.017

FIG. 3. Haplotype features in an LD block between SNP-25 and SNP-13 with frequencies. The *numbers 1* and *2* indicate major allele and minor allele, respectively. CONT, Control.

tivity as did the wild-type HIF-1α. The results show consistently higher HIF-1α transcription activity in cells transfected with mutant S582 than with wild-type HIF-1α. However, enhanced transactivation capacity of the S582 HIF-1α mutant was observed with statistical significance only under hypoxic condition ($P = 0.012$) (Fig. 4).

Discussion

The estimated prevalence of diabetes in Japan is 13 million, 90% with T2DM as a result of both environmental and genetic factors. So far, only genetic variants of the Calpain-10 gene (19), PPARγ gene (20), and Kir 6.2 gene (21) have been reported to be related to the occurrence of T2DM in large studies, and genes including angiotensin converting enzyme (ACE), aldose reductase (AR), nitric oxide synthase (NOS), VEGF, and paraoxonase 1 (PON1) *etc.* have been reported to contribute to the development of diabetic retinopathy (22).

We previously compared the expression profile of 1000 mRNAs of rat pancreatic islets with those of rat retina, resulting in the identification of 123 commonly expressed genes. These genes are candidates in both development of T2DM and diabetic retinopathy (23). One of them, VEGF, was

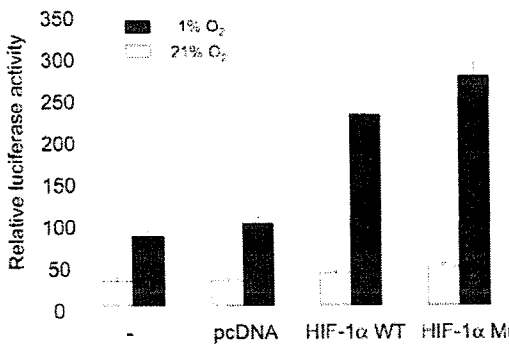

FIG. 4. Transactivation capacity of mutant S582 HIF-1α. Transcription activity with no vector, empty vector, wild type, and P582S HIF-1α (500 ng) was analyzed by cotransfection assay using reporter vector VEGF promoter-pGL3 (200 ng/35-mm well) and a Renilla-luciferase (25 ng/35-mm well) as internal control. The average of three independent experiments is shown (*bar*, ±SD).

reported to be a susceptibility gene for both onset of diabetes and diabetic retinopathy (6, 7), and HIF-1α was reported to induce expression predominantly of VEGF and other important genes involved in glucose metabolism under hypoxic condition, leading us to examine the correlation between HIF-1 and T2DM and retinopathy more closely.

In this study, we examined 38 kb covering the entire coding region of the HIF-1α gene in 16 Japanese subjects and identified a total of 35 genetic variations. Thirty-two SNPs were identified in noncoding regions, and three SNPs were identified in coding regions. We defined haplotypes by all possible pairs of 10 SNPs, based on the LD pattern estimated using the frequent SNPs, and examined the associations with T2DM and retinopathy. The haplotype comprising SNP-25 and SNP-13 was most significantly associated with T2DM. cSNP-10 (P582S) was significantly associated with decreased risk of T2DM. Interestingly, the rare allele cSNP-10, resulting in S582, was completely assigned on the 2-2 haplotype comprising SNP-25 and SNP-13, which was observed at significantly higher frequency in control subjects. Thus, the S582 HIF-1α mutant could be protective against the onset of T2DM.

The progress of diabetic retinopathy is known to reflect the duration of diabetes, control of blood glucose level, insulin dosage, and blood pressure. The percentage of patients treated with insulin and hypertension drugs was higher in the group with retinopathy, consistent with previous studies, although the P582S HIF-1α mutation was not associated with onset of diabetic retinopathy even after logistic regression analysis.

The same P582S HIF-1α somatic mutation was found in one of five androgen-independent prostate cancer samples in a recent study, although the mutant was not functionally characterized (24). In addition, an HIF-1α polymorphism, P582S, was identified in a study of renal cell cancers, but the significance in renal cell cancer patients and controls differs in two studies (25, 26). Recently, a P582S HIF-1α mutation was identified in prostate cancer and was reported to enhance transcriptional activity as a result of increased stability under normoxic conditions, resulting in increased tumor microvessel density (27, 28). Proline 582 has not been identified as a site for HIF-1α hydroxylation and is not known to mediate VHL binding. Moreover, the substitution of serine for proline in this position does not appear to prevent VHL binding *in vitro* to a fragment of HIF-1α after hydroxylation at proline 564 (29) Thus, if proline 582 is not a target for hydroxylation, conformational changes induced by the proline to serine substitution could influence hydroxylation at other sites as well as degradation *in vivo*.

HIF-1α is an important inducing factor of VEGF, a key factor in angiogenesis of islets in the pancreatic developmental stage in determining β-cell mass and properties (7), although a high expression level of HIF-1α is observed in hypoxic human adult pancreatic islets and is reported to be correlated with apoptosis (30). In the present study in HEK293 renal cells, the mutant S582 showed a consistently higher level of HIF-1α transcriptional activity than in wild type, and the enhanced transactivation capacity of the mutant was observed with statistical significance only under hypoxic conditions. Accordingly, polymorphism P582S, by enhancing the transcriptional activity of target genes, could be a protective factor against onset of T2DM by its activities in the pancreatic developmental stage. When the two groups with and without S582 are compared, there are no significant differences in

TABLE 2. Association study using frequent SNPs in *HIF1A* in patients with T2DM and controls

SNP name	Frequencies of minor allele			Frequencies of genotype		T2DM *vs.* control	
	T2DM (n = 440)	Control (n = 572)		T2DM (n = 440)	Control (n = 572)	χ^2	*P*
SNP30	0.144	0.141	W/W	0.736	0.754	0.042	0.837
			W/M	0.240	0.211		
			M/M	0.024	0.035		
SNP31	0.06	0.065	W/W	0.892	0.890	0.195	0.658
			W/M	0.096	0.090		
			M/M	0.012	0.020		
SNP1	0.073	0.072	W/W	0.857	0.859	0.007	0.934
			W/M	0.138	0.138		
			M/M	0.004	0.004		
SNP2	0.127	0.133	W/W	0.759	0.746	0.134	0.714
			W/M	0.228	0.243		
			M/M	0.013	0.011		
SNP3	0.186	0.2	W/W	0.670	0.648	0.553	0.457
			W/M	0.286	0.304		
			M/M	0.043	0.048		
SNP4	0.145	0.147	W/W	0.729	0.733	0.007	0.932
			W/M	0.251	0.241		
			M/M	0.020	0.027		
SNP5	0.146	0.136	W/W	0.725	0.748	0.392	0.532
			W/M	0.257	0.231		
			M/M	0.018	0.021		
SNP6(S28Y)	0.009	0.014	W/W	0.983	0.972	1.141	0.285
			W/M	0.017	0.028		
			M/M	0	0		
SNP25	0.188	0.222	W/W	0.664	0.613	3.465	0.063
			W/M	0.296	0.331		
			M/M	0.040	0.056		
SNP7	0.196	0.225	W/W	0.650	0.606	2.481	0.115
			W/M	0.307	0.338		
			M/M	0.042	0.056		
SNP8	0.148	0.148	W/W	0.721	0.722	0	0.996
			W/M	0.261	0.259		
			M/M	0.018	0.019		
SNP9	0.416	0.429	W/W	0.345	0.312	0.32	0.572
			W/M	0.477	0.518		
			M/M	0.178	0.170		
SNP10(P582S)	0.041	0.073	W/W	0.918	0.863	8.925	**0.003**
			W/M	0.082	0.127		
			M/M	0	0.010		
SNP11(A588T)	0.047	0.044	W/W	0.908	0.917	0.141	0.708
			W/M	0.090	0.080		
			M/M	0.002	0.004		
SNP14	0.126	0.129	W/W	0.760	0.752	0.038	0.846
			W/M	0.228	0.238		
			M/M	0.011	0.009		
SNP15	0.424	0.431	W/W	0.326	0.306	0.12	0.729
			W/M	0.501	0.525		
			M/M	0.173	0.169		
SNP16	0.126	0.129	W/W	0.760	0.752	0.038	0.846
			W/M	0.228	0.238		
			M/M	0.011	0.009		
SNP17	0.126	0.129	W/W	0.760	0.752	0.038	0.846
			W/M	0.228	0.238		
			M/M	0.011	0.009		
SNP18	0.122	0.128	W/W	0.770	0.758	0.194	0.66
			W/M	0.217	0.227		
			M/M	0.013	0.015		
SNP20	0.173	0.199	W/W	0.690	0.643	2.14	0.143
			W/M	0.273	0.316		
			M/M	0.037	0.041		
SNP12	0.135	0.132	W/W	0.742	0.746	0.061	0.804
			W/M	0.245	0.245		
			M/M	0.013	0.009		
SNP13	0.211	0.222	W/W	0.615	0.605	0.314	0.575
			W/M	0.347	0.345		
			M/M	0.038	0.049		
SNP28	0.327	0.335	W/W	0.470	0.465	0.16	0.69
			W/M	0.407	0.400		
			M/M	0.123	0.135		
SNP29	0.109	0.097	W/W	0.799	0.822	0.768	0.381
			W/M	0.183	0.161		
			M/M	0.017	0.017		

P value < 0.05 is shown in *bold*. M, Mutant; W, wild type.

Original Article

A Functional Variant in the Human Betacellulin Gene Promoter Is Associated With Type 2 Diabetes

Yoshio Nakano,[1] Hiroto Furuta,[1] Asako Doi,[1] Shohei Matsuno,[1] Takayuki Nakagawa,[1] Hiroko Shimomura,[1] Setsuya Sakagashira,[1] Yukio Horikawa,[2] Masahiro Nishi,[1] Hideyuki Sasaki,[1] Tokio Sanke,[3] and Kishio Nanjo[1]

Betacellulin (BTC) plays an important role in differentiation, growth, and antiapoptosis of pancreatic β-cells. We characterized about 2.3 kb of the 5′-flanking region of human *BTC* gene and identified six polymorphisms (−2159A>G, −1449G>A, −1388C>T, −279C>A, −233G>C, and −226A>G). The G allele in the −226A>G polymorphism was more frequent in type 2 diabetic patients (n = 250) than in nondiabetic subjects (n = 254) (35.6% vs. 27.8%, P = 0.007), and the −2159G, −1449A, and −1388T alleles were in complete linkage disequilibrium with the −226G allele. The frequencies of the −279A and −233C alleles were low (7.0 and 2.0% in diabetic patients), and no significant differences were observed. In the diabetic group, insulin secretion ability, assessed by the serum C-peptide response to intravenous glucagon stimulation, was lower in patients with the −226G allele (G/G, 2.96 ± 0.16 ng/ml; G/A, 3.65 ± 0.18 ng/ml; A/A, 3.99 ± 0.16 ng/ml at 5 min after stimulation; P = 0.008). Furthermore, in vitro functional analyses indicated that both the −226G and the −233C alleles caused an ~50% decrease in the promoter activity, but no effects of the −2159A>G, −1449G>A, −1388C>T, and −279C>A polymorphisms were observed. These results suggest that the −226A/G polymorphism of the *BTC* gene may contribute to the development of diabetes. *Diabetes* 54:3560–3566, 2005

Impaired insulin secretion and insulin resistance are major defects observed in type 2 diabetic patients. When it becomes impossible for pancreatic β-cells to secrete the amount of insulin corresponding to the demand in peripheral tissues, blood glucose levels are elevated in diabetic patients. This insufficient insulin secretion is associated with an insufficient β-cell mass in the pancreatic islet and/or functional defects of the β-cells. Several recent reports have shown the importance of the β-cell mass in the pathophysiology of type 2 diabetes (1–4). Regulation of the β-cell mass appears to involve a balance of β-cell replication, neogenesis (the development of new islets from pancreatic ducts), and apoptosis. Some factors that are associated with the regulation of the β-cell mass have been identified (5), and we hypothesized that functional gene polymorphisms in these factors might be associated with the development of diabetes.

Betacellulin (BTC), a member of the epidermal growth factor (EGF) family, was purified from the conditioned medium of a cell line derived from mouse pancreatic β-cell tumors (6). Its primary translational product was composed of 178 amino acid residues, which contained a signal sequence, transmembrane, and cytoplasmic domains in addition to an EGF-like domain (7). The expression of BTC is predominantly found in the pancreas and in the intestine (8). In particular, BTC is expressed in α-, β-, and duct cells in a normal adult pancreas and in primitive duct cells of the fetal pancreas (9). BTC converts the rat pancreatic acinar cell line (AR42J cells) to insulin-expressing cells together with activin A (10) and has the potential for the growth of a rat insulinoma cell line, INS-1 cells (11). BTC promotes the neogenesis of β-cells and accelerates the improvement of glucose tolerance in mice with diabetes induced by selective alloxan perfusion (12). BTC also improves glucose metabolism by promoting the conversion of intraislet precursor cells to β-cells in streptozotocin-treated mice (13). Furthermore, the activation of the EGF receptor by BTC induces an inhibitory effect on apoptosis (14). These observations suggest that BTC plays an important role in differentiation, growth, and antiapoptosis of the pancreatic β-cells.

We previously screened gene polymorphisms in the protein coding exons of the human *BTC* gene in type 2 diabetic patients (15). The frequencies of polymorphisms identified, however, were similar between the diabetic patients and the control subjects. In this study, to examine the role of polymorphisms in the promoter of the human *BTC* gene, we characterized the 5′-flanking region of the human *BTC* gene and screened gene polymorphisms in the promoter in type 2 diabetic patients.

RESEARCH DESIGN AND METHODS

Characterization of the 5′-flanking region of the human *BTC* gene. To assess the portions of the 5′-flanking region of the human *BTC* gene required for promoter activity, a series of deletions of the region were fused to a luciferase reporter gene. The 5′-flanking regions of the human *BTC* gene spanning −2,330 to 160 bp, −881 to 160 bp, −669 to 160 bp, −350 to 160 bp, and −152 to 160 bp numbered relative to the translation start site, were amplified by PCR using Pfu DNA polymerase (Stratagene, La Jolla, CA), and were subcloned into the *Sma*I site of pGL3-basic firefly luciferase reporter vector (Promega, Madison, WI) in the 5′-3′ orientation. The sequences of constructs were confirmed by bidirectional sequencing. We transiently trans-

From [1]The First Department of Medicine, Wakayama Medical University, Wakayama, Japan; the [2]Department of Diabetes and Endocrinology, Gifu University School of Medicine, Gifu, Japan; and the [3]Department of Clinical Laboratory Medicine, Wakayama Medical University, Wakayama, Japan.

Address correspondence and reprint requests to Hiroto Furuta, MD, PhD, The First Department of Medicine, Wakayama Medical University, 811-1 Kimiidera, Wakayama 641-8509, Japan. E-mail: hfuruta@wakayama-med.ac.jp.

Received for publication 2 June 2005 and accepted in revised form 23 August 2005.

Additional information for this article can be found in an online appendix at http://diabetes.diabetesjournals.org.

BTC, betacellulin; CPR, C-peptide response; EGF, epidermal growth factor.

TABLE 1
Clinical characteristics of the subjects enrolled in the present study

	Nondiabetic subjects	Type 2 diabetic patients
n (male/female)	254 (67/187)	250 (135/115)
Age (years)	75.1 ± 8.0	63.1 ± 11.3
BMI (kg/m^2)	21.8 ± 3.7	23.5 ± 3.2
A1C (%)	5.0 ± 0.4	7.4 ± 1.3
Age at diagnosis (years)	—	45.5 ± 9.4
Mode of treatment (D/OHA/Ins) (%)	—	18.8/40.8/40.4

Data are means ± SD unless otherwise indicated. D, diet; Ins, insulin; OHA, oral hypoglycemic agent.

fected 0.1 μg each of these constructs with 0.01 μg pRL-SV40 vector (renilla luciferase under control of SV40 promoter), as an internal control for transfection efficiency, into βTC3 cells using FuGENE6 transfection reagent (Roche Diagnostics, Mannheim, Germany). The βTC3 cells were seeded into 12-well culture plates and were maintained in Dulbecco's modified Eagle's medium containing 4,500 mg/l glucose, 10% fetal bovine serum, and antibiotics (100 units/ml penicillin G sodium and 100 mg/ml streptomycin sulfate). After 48 h, we collected the cells and measured luciferase activity using Dual-luciferase Reporter Assay System (Promega). The relative luciferase activity for each construct was calculated as a fold increase over the activity for the promoterless control vector (pGL3-basic). The data presented represent the means of three independent transfection experiments per construct.

Screening and genotyping of polymorphisms in the promoter region of the human *BTC* gene. About 2.3 kb of the promoter region was amplified with a PCR and sequenced in DNA samples from 20 Japanese type 2 diabetic patients. PCR was carried out using AmpliTaq Gold polymerase (Applied Biosystems, Foster City, CA). Sequencing was carried out using Big Dye Terminator Cycle Sequencing FS Ready Reaction kit (Applied Biosystems) on an automated DNA capillary sequencer (model 310; Applied Biosystems). Polymorphisms identified in this screening were designated according to their location from the translation start site. Sequence information of the primers and the conditions for PCR-direct sequencing are shown in Supplemental Table 1 in the online appendix (available at http://diabetes.diabetesjournals.org).

Polymorphisms identified were genotyped in 250 Japanese type 2 diabetic patients and 254 nondiabetic subjects using PCR direct sequencing. We calculated linkage disequilibrium coefficients (D′ and Δ^2) using the Graphical Overview of Linkage Disequilibrium program (http://www.sph.umich.edu/csg/abecasis/GOLD). All of the type 2 diabetic patients in this study were recruited from patients attending the outpatient clinic of the Wakayama Medical University Hospital. All patients were evaluated for their insulin secretion ability by the serum C-peptide immunoreactivity response (CPR) to intravenous glucagon stimulation. Because renal function affects serum CPR levels, patients with an elevated serum creatinine level (>1.2 mg/dl) were not included. Diabetes was diagnosed according to the criteria of the World Health Organization, and patients who were glutamic acid decarboxylase antibody positive and/or had started insulin therapy within 3 years of the diagnosis of diabetes were excluded from this study. Nondiabetic subjects were chosen using the following criteria: age of >60 years, HbA_{1c} (A1C) of <5.6%, fasting plasma glucose of <110 mg/dl, and no family history of diabetes. The clinical characteristics of type 2 diabetic patients and nondiabetic subjects are shown in Table 1. All of the participants gave their written informed consent before participating in the study. This study was approved by the ethics committee of the Wakayama Medical University.

Assessment of the insulin secretion ability in type 2 diabetic patients. We assessed the insulin secretion ability in type 2 diabetic patients using their serum CPR response to intravenous glucagon stimulation (16). After an overnight fast, glucagon (1 mg/body) was injected intravenously, and serum CPR levels were measured before (CPR0′) and 5 min after (CPR5′) injection, and then, the increment of CPR for 5 min (ΔG5′) was calculated. The patients treated with drugs were instructed not to take their morning oral hypoglycemic agents or insulin on the day of test.

Functional properties of polymorphisms on the promoter activity of the human *BTC* gene. The −279C>A, −233G>C, and −226A>G gene polymorphisms were introduced into the pGL3-reporter vector containing the 5′-flanking region spanning from −669 to 160 bp using QuikChange site-directed mutagenesis kit (Stratagene) for generating five constructs, pGL3-(−669/160)CGA, pGL3-(−669/160)CGG, pGL3-(−669/160)AGA, pGL3-(−669/160)CCA, and pGL3-(−669/160)CCG. Four gene polymorphisms, −2159A>G, −1449G>A, −1388C>T, and −226A>G, were also introduced into the pGL3-reporter vector containing the 5′-flanking region spanning from −2,330 to 160 bp using the same kit for generating three constructs, pGL3-(−2330/160)AGCA, pGL3-(−2330/160)GATA, and pGL3-(−2330/160)GATG. These constructs were transfected into the βTC3 cells, and the relative luciferase activity for each construct was calculated as described above.

Statistical analysis. Results are presented as means ± SE unless otherwise indicated. The proportion of genotypes or alleles was compared by a χ^2 test. Group differences of continuous variables were compared using an unpaired *t* test or a one-way ANOVA followed by a post hoc analysis with a Fisher's protected least-significant difference test. Categorical variables were compared with a χ^2 test. The data of serum CPR levels were log transformed before analyzing. These analyses were performed with the StatView program for Windows (version 5.01; SAS Institute, Cary, NC). A *P* value of <0.05 was considered to be statistically significant.

RESULTS

Characterization of the 5′-flanking region of the human *BTC* gene. The relative luciferase activities of the reporter constructs in the βTC3 cells are shown in Fig. 1. The construct containing from −350 to 160 bp demonstrated a fivefold increase in activity compared with the promoterless construct ($P < 0.001$), whereas only background activity was obtained with the construct containing from −152 to 160 bp. Furthermore, a significant increase in activity was observed with the addition of the region between −669 and −350 bp ($P = 0.020$). Conversely, the further addition of the region between −881 and −669 bp attenuated the promoter activity ($P = 0.002$). Finally, the promoter activity of the construct containing the region up to −2,330 bp was significantly higher than that of the construct containing the region up to −669 bp ($P < 0.001$). These data suggest that the basal promoter of the human *BTC* gene is located within the −200-bp region between −350 and −152 bp relative to the translation start site, the positive regulatory elements are located within the regions between −669 and −350 bp and between −2,330 and −881 bp, and the negative regulatory element(s) is located within the region between −881 and −669 bp.

Polymorphisms in the promoter region of the human *BTC* gene. About 2.3 kb of the promoter region was screened in 20 Japanese type 2 diabetic patients, and six polymorphisms were identified. These polymorphisms include a G for A substitution at −2,159 bp (−2159A>G), an A for G substitution at −1,449 bp (−1449G>A), a T for C substitution at −1,388 bp (−1388C>T), an A for C substitution at −279 bp (−279C>A), a C for G substitution at −233 bp (−233G>C), and a G for A substitution at −226 bp (−226A>G). All polymorphisms were numbered relative to the translation start site. The reference single nucleotide polymorphism ID numbers of −2159A>G, −1449G>A, −1388C>T, and −226A>G are rs11733938, rs13121979, rs13101336, and rs2278862, respectively.

We genotyped these polymorphisms in 250 type 2 diabetic patients and 254 nondiabetic subjects. The allelic distributions were in the Hardy-Weinberg equilibrium expectations, and the −2159G, −1449A, −1388T, and −226G alleles were in complete linkage disequilibrium with each other (D′ = 1.00, Δ^2 = 1.00). For the −226A>G polymorphism, the G allele was significantly more frequent in type 2 diabetic patients than in nondiabetic subjects ($P = 0.007$). The odds ratios (OR) of subjects with the G/G or A/G genotype were 1.90 (95% CI 1.05–3.41, $P = 0.031$) and 1.49 (1.02–2.16, $P = 0.038$) compared with those having the A/A genotype, respectively. In the −279C>A and −233G>C polymorphisms, no significant differences were observed

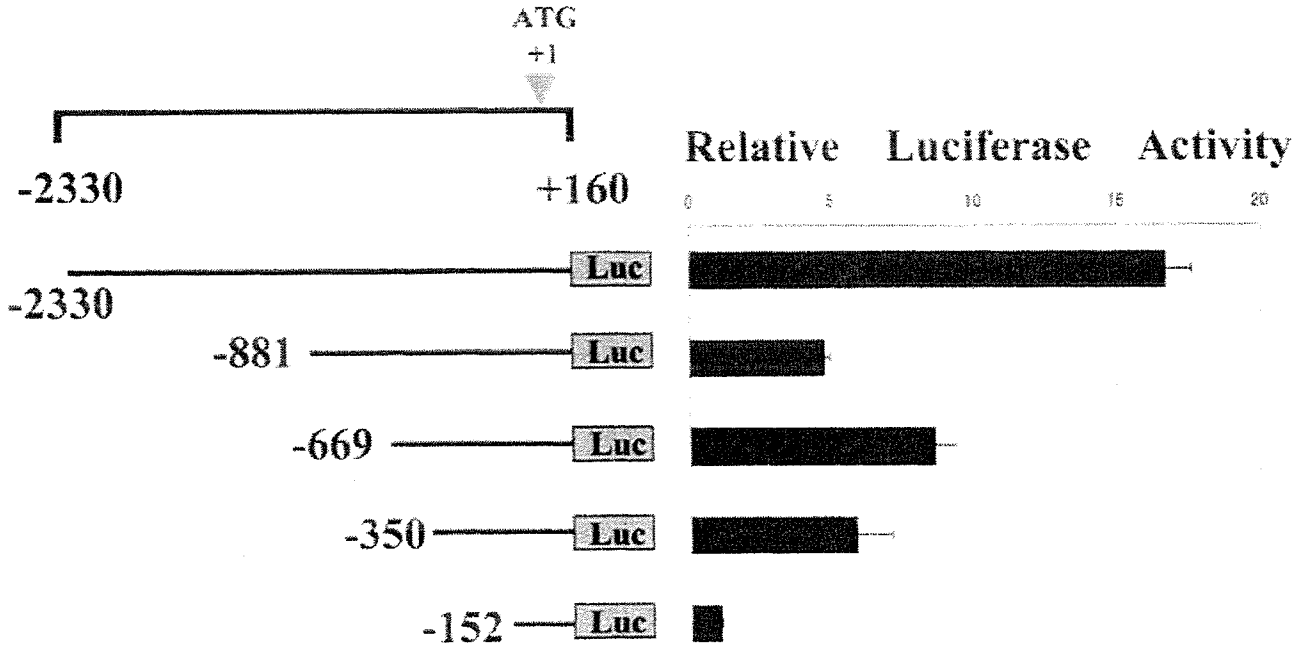

FIG. 1. Deletion analysis of the 5′-flanking region of the human *BTC* gene. The 5′-flanking region was progressively deleted, fused to a firefly luciferase reporter (pGL3-basic) vector, and transfected into βTC3 cells. Cells were cotransfected with a *Renilla* luciferase control (pRL-SV40) vector. The firefly luciferase activity of each construct was normalized in comparison with coexpressed *Renilla* luciferase activity and expressed as the fold increase relative to the activity of the promoterless pGL3-basic vector. All constructs are numbered relative to the translation start site. The data presented represent the means of three independent transfection experiments per construct. Data are means ± SE. The differences in the averaged activities were compared using a one-way ANOVA followed by post hoc test.

in genotypic and allelic distribution between diabetic patients and nondiabetic subjects (Table 2).

Relationship between the −226A>G polymorphism and the insulin secretion ability in type 2 diabetic patients. As shown in Table 3, there were no significant differences in sex, age, age at diagnosis of diabetes, duration of diabetes, maximum BMI, and present BMI among the three groups of type 2 diabetic patients according to the −226A>G genotypes. However, the insulin secretion ability evaluated by the serum CPR response to glucagon stimulation was significantly lower in patients with the G allele (G/G, 2.96 ± 0.16 ng/ml; G/A, 3.65 ± 0.18 ng/ml; and A/A, 3.99 ± 0.16 ng/ml for CPR5′; $P = 0.008$ by ANOVA. G/G, 1.39 ± 0.11 ng/ml; G/A, 1.87 ± 0.11 ng/ml; and A/A, 2.13 ± 0.11 ng/ml for ΔG5′; $P = 0.002$.) (Fig. 2). The fasting serum CPR levels were also lower in patients with the G allele (G/G, 1.58 ± 0.10 ng/ml; G/A, 1.76 ± 0.07 ng/ml; and A/A, 1.86 ± 0.07 ng/ml; $P = 0.182$), and the A1C levels and the percentage of patients with insulin treatment were higher in patients with the G allele, but these differences were not statistically significant.

Effects of polymorphisms on the promoter activity of the human *BTC* gene. To investigate whether the −279C>A, −233G>C, and −226A>G gene polymorphisms would affect the promoter activity of the human *BTC* gene, we constructed four plasmids containing the 5′-flanking region spanning from −669 to 160 bp, pGL3-(−669/160)CGA, pGL3-(−669/160)CGG, pGL3-(−669/160)AGA, and pGL3-(−669/160)CCA vectors. In transient transfection into the βTC3 cells, the pGL3-(−669/160)CGA vector induced luciferase activity sevenfold greater, relative to the promoterless pGL3-basic vector (Fig. 3). On the other hand, the pGL3-(−669/160)CGG vector had an ~50% decrease in the activity compared with the pGL3-(−669/

TABLE 2
Comparison of genotypic and allelic distributions of gene polymorphisms between type 2 diabetic patients and nondiabetic subjects

Polymorphisms	Genotypes				Alleles		
−226A>G	A/A	A/G	G/G		A	G	
Type 2 diabetes	106 (42.4)	110 (44.0)	34 (13.6)	$P = 0.032$	322 (64.4)	178 (35.6)	$P = 0.007$
Nondiabetic	136 (53.5)	95 (37.4)	23 (9.1)		367 (72.2)	141 (27.8)	
−233G>C	G/G	G/C	C/C		G	C	
Type 2 diabetes	240 (96.0)	10 (4.0)	0 (0)	$P = 0.439$	490 (98.0)	10 (2.0)	$P = 0.419$
Nondiabetic	247 (97.2)	7 (2.8)	0 (0)		501 (98.6)	7 (1.4)	
−279C>A	C/C	C/A	A/A		C	A	
Type 2 diabetes	215 (86.0)	35 (14.0)	0 (0)	$P = 0.643$	465 (93.0)	35 (7.0)	$P = 0.655$
Nondiabetic	222 (87.4)	32 (12.6)	0 (0)		476 (93.7)	32 (6.3)	

Data are *n* (%). The results of −2159A>G, −1449G>A, and −1388C>T are not shown because the −2159G, −1449A, and −1388T alleles are in complete linkage disequilibrium with the −226G allele.

TABLE 3
Clinical characteristics and biochemical data of type 2 diabetic patients classified according to their genotypes of the −226A>G polymorphism

	−226A >G genotype			
	G/G	G/A	A/A	*P*
n (male/female)	34 (16/18)	110 (58/52)	106 (61/44)	0.488
Age (years)	62.4 ± 2.0	64.3 ± 1.1	62.2 ± 1.1	0.377
Age at diagnosis (years)	45.6 ± 1.5	45.4 ± 0.9	45.6 ± 1.0	0.976
Duration of diabetes (years)	16.7 ± 1.8	18.6 ± 1.0	16.4 ± 1.0	0.265
Maximum BMI (kg/m^2)	27.0 ± 0.6	26.5 ± 0.3	27.0 ± 0.3	0.554
BMI (kg/m^2)	23.4 ± 0.5	23.3 ± 0.3	23.7 ± 0.3	0.662
A1C (%)	7.7 ± 0.2	7.5 ± 0.1	7.2 ± 0.1	0.072
Mode of treatment (D/OHA/Ins) (*n*)	6/11/17	18/47/45	23/44/39	
Insulin (%)	50.0	40.9	37.7	0.389

Data are shown as means ± SE unless otherwise indicated. *P* values are compared by one-way ANOVA or χ^2 test for existence of insulin treatment. D, diet; Ins, insulin; OHA, oral hypoglycemic agents.

160)CGA vector (3.84 ± 0.23 vs. 6.98 ± 0.33, $P < 0.001$). Furthermore, the pGL3-(−669/160)CCA vector had an ~50% decrease in the activity compared with the pGL3-(−669/160)CGA vector (3.73 ± 0.23 vs. 6.98 ± 0.33, $P < 0.001$). The relative luciferase activity of the pGL3-(−669/160)AGA vector was similar to that of the pGL3-(−669/160)CGA vector (7.30 ± 0.43 vs. 6.98 ± 0.33, $P = 0.533$). Because not only the −226A>G polymorphism but also the −233G>C polymorphism affected the promoter activity of the human *BTC* gene, we further constructed pGL3-(−669/160)CCG vector, but the relative luciferase activity of the pGL3-(−669/160)CCG vector was similar to those of the pGL3-(−669/160)CGG and pGL3-(−669/160)CCA vectors. We next examined the effect of −2159A>G, −1449G>A, and −1388C>T polymorphisms on the promoter activity of the human *BTC* gene, because the −226G allele was in complete linkage disequilibrium with −2159G, −1449A, and −1388T alleles. Four polymorphisms, −2159A>G, −1449G>A, −1388C>T, and −226A>G, were introduced into pGL3-reporter vector containing the 5′-flanking region spanning from −2,330 to 160 bp for generating three plasmids, pGL3-(−2330/160)AGCA, pGL3-(−2330/160)GATA, and pGL3-(−2330/160)GATG. The pGL3-(−2330/160)GATA vector induced luciferase expression ~14-fold greater, relative to the promoterless pGL3-basic vector, and the pGL3-(−2330/160)GATG had an ~50% decrease in activity compared with the pGL3-(−2330/160)GATA vector (14.4 ± 1.20 vs. 8.02 ± 0.50, $P < 0.001$) (Fig. 4). On the other hand, the relative luciferase activity of the pGL3-(−2330/160)GATA vector was similar to that of the pGL3-(−2330/160)AGCA vector (14.4 ± 1.20 vs. 16.4 ± 0.81, $P = 0.131$). These results suggest that −2159A>G, −1449G>A, and −1388C>T polymorphisms do not affect the transcription of the human *BTC* gene.

DISCUSSION

In this study, our purpose was to investigate the role of gene polymorphisms in the promoter of the human *BTC* gene in type 2 diabetic patients. Because the promoter of the human *BTC* gene had not been well studied, we initially characterized about 2.3 kb of the 5′-flanking region of the human *BTC* gene in a pancreatic β-cell line. We then screened gene polymorphisms in this region and found that the G allele of the −226A>G polymorphism was more frequent in type 2 diabetic patients than in nondiabetic subjects. However, the possibility that this

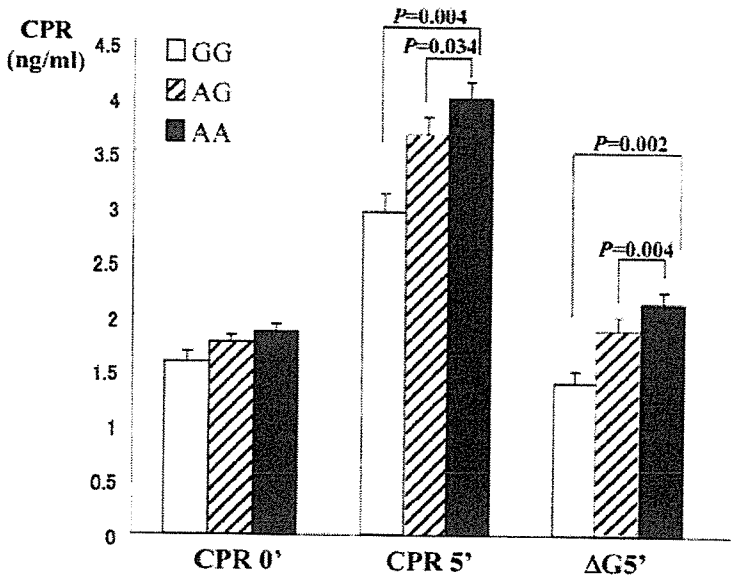

FIG. 2. The effect of the −226A>G polymorphism on fasting C-peptide immunoreactivity (CPR) levels and CPR response to glucagon stimulation in type 2 diabetic patients. The serum CPR levels at 5 min after injection (CPR 5′) and the increment of CPR for 5 min (ΔG5′ = CPR 5′ − CPR 0′) were significantly lower in patients with the G allele. Data are means ± SE. The differences in the averaged CPR levels were compared using a one-way ANOVA followed by post hoc test.

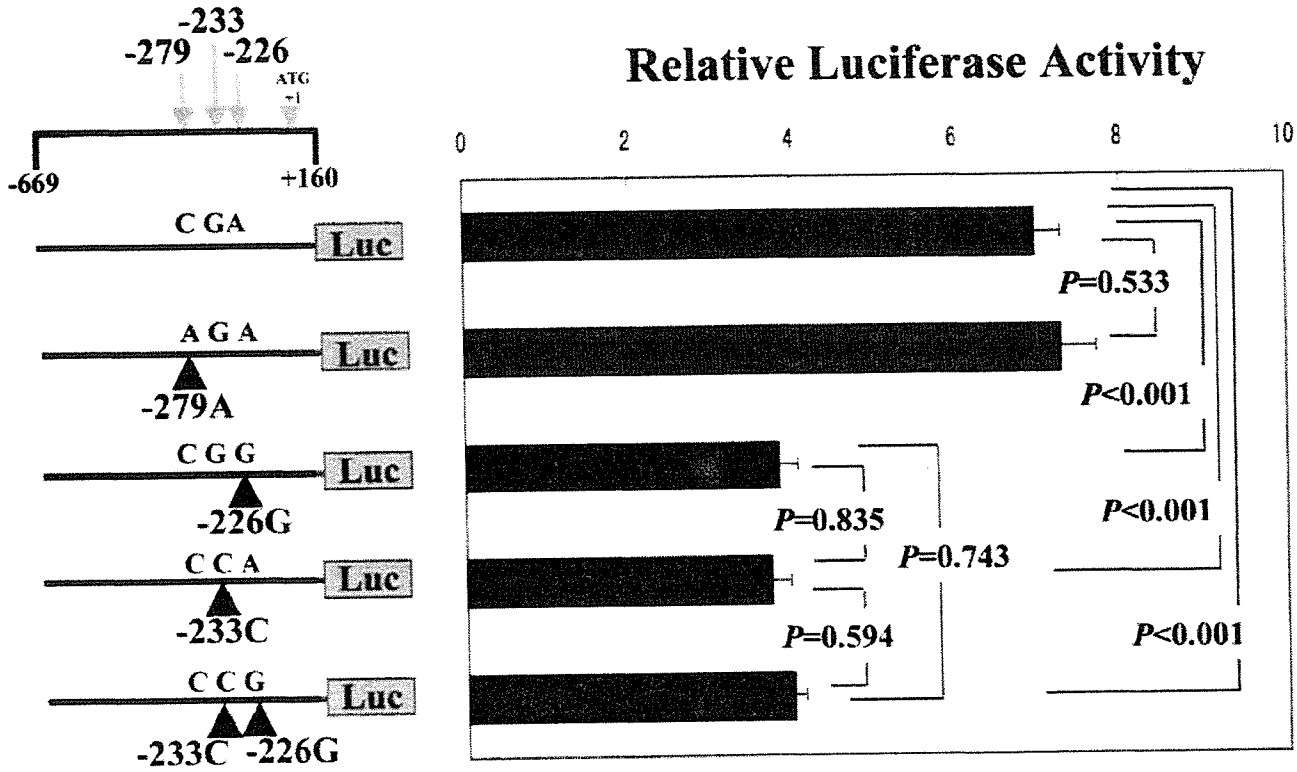

FIG. 3. The effects of the −279C>A, −233G>C, and −226A>G polymorphisms on the promoter activity of the human *BTC* gene. Five plasmids containing the 5′-flanking region, spanning from −669 to 160 bp, with each of five different combinations for the −279C>A, −233G>C, and −226A>G polymorphisms upstream of a luciferase gene transcriptional unit were constructed and transiently transfected into the βTC3 cells. The data presented represent the means of three independent transfection experiments per construct. Data are means ± SE. The differences in the averaged activities were compared using a one-way ANOVA followed by post hoc test.

result is a false-positive finding should be considered, because the sample size of our case-control analysis is small and the *P* values obtained are modest (17). Therefore, we further investigated the effect of the −226A>G polymorphism on clinical profiles of patients and the functional properties of all polymorphisms identified. We first examined the relationship between the G allele of the −226A>G polymorphism and insulin secretion ability in type 2 diabetic patients, because BTC plays an important role in differentiation, growth, and antiapoptosis of the pancreatic β-cells (10–14). Glucagon is a potent stimulus for the pancreatic β-cells, and the serum CPR to intravenous glucagon stimulation has been used to evaluate residual insulin secretion in diabetic patients (16,18). We, therefore, used this test to evaluate the insulin secretion ability in our patient group and observed that the serum CPR to glucagon was significantly lower in patients with the G allele. On the other hand, the A1C level was higher, but not significantly so, in patients with the G allele. The chronic hyperglycemia itself also causes the impairment of β-cell function. However, we think that this may not affect the result, because it has been reported that the serum CPR to glucagon was little influenced by the chronic hyperglycemia (16,19). Moreover, although an influence of oral hypoglycemic agents on the serum CPR should be considered, the percentages of patients treated with oral drugs were almost similar among the groups (G/G, 32%; G/A, 42.7%; A/A, 41.5%; $P = 0.550$). We next examined the functional properties of polymorphisms. A promoter with the −226G allele had an ~50% decrease in the activity. The −226G allele was also in complete linkage disequilibrium with the −2159G, −1449A, and −1338T alleles, but no effects of the −2159A>G, −1449G>A, and −1388C>T polymorphisms on the promoter activity were observed. Furthermore, although we could not observe significant difference in the frequency of −233C allele in our case-control study, a promoter with the −233C allele also had an ~50% decrease in the activity. The −233C allele frequency was only 2.0% in diabetic patients and 1.4% in nondiabetic subjects. The power of our study may be not enough to detect the difference in case-control analysis because of the low frequency of C allele. In subjects with the G/C genotype on the −233G>C polymorphism, 6 of 10 subjects in diabetic group and 2 of 7 subjects in nondiabetic group had the A/G genotype on the −226A>G polymorphism. Subjects with the G/G genotype on the −226A>G polymorphism were not observed in both groups. On the basis of these results, we conclude that a decreased expression of BTC may be associated with the development of type 2 diabetes.

BTC is a member of the EGF family. The addition of BTC promoted proliferation, regeneration, and neogenesis of pancreatic β-cells in both a cell line (11) and diabetic mice developed by treatment with the β-cell toxin (12,13). Furthermore, BTC has an antiapoptotic effect via transactivation of the EGF receptors, and the effect is greater than that by EGF (14). Several reports suggest that a decreased β-cell mass is observed in type 2 diabetic patients (1–4) and plays an important role in the pathogenesis of type 2 diabetes. The β-cell mass is regulated by a balance be-

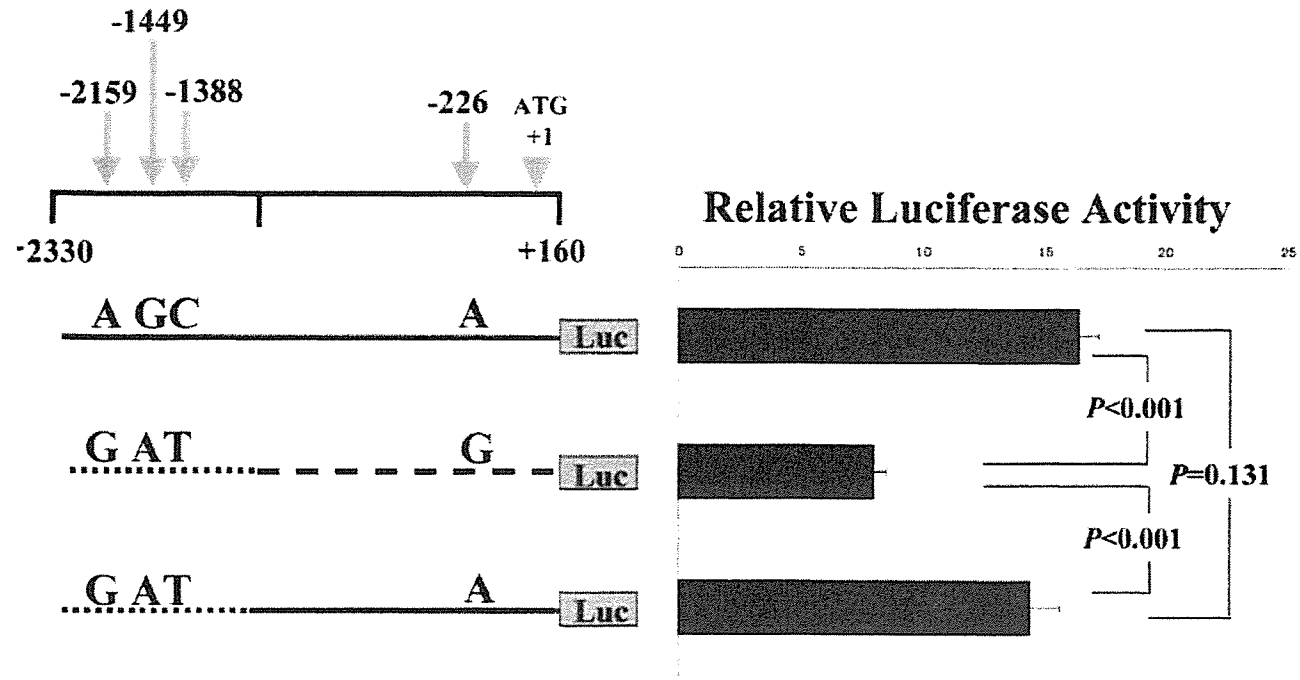

FIG. 4. The effects of the −2159A>G, −1449G>A, and −1388C>T polymorphisms on the promoter activity of the human *BTC* gene. Three plasmids containing the 5′-flanking region, spanning from −2,330 to 160 bp, with each of three different combinations for the −2159A>G, −1449G>A, −1388C>T, and −226A>G polymorphisms upstream of a luciferase gene transcriptional unit were constructed and transiently transfected into the βTC3 cells. No effects of the −2159A>G, −1449G>A, and −1388C>T polymorphisms in the promoter activity were observed. The data presented represent the means of three independent transfection experiments per construct. Data are means ± SE. The differences in the averaged activities were compared using a one-way ANOVA followed by post hoc test.

tween an input (β-cell neogenesis from pancreatic ducts and β-cell replication within islets) and an output (β-cell apoptosis). Because BTC accelerates the input and decelerates the output, a decreased expression of BTC affected by gene polymorphism may accelerate a decrease in β-cell mass in type 2 diabetic patients. *BTC*-null mice have been generated by gene targeting (20). The mice were viable and grew normally. No morphological changes were observed in the newborn pancreases; also, adult $BTC^{+/-}$ and $BTC^{-/-}$ males responded similarly to glucose challenge tests. Their actual data, however, were not shown in the report. In addition to the BTC dysfunction, other genetic and environmental factors, including aging, may be required for the development of overt diabetes.

The sequences surrounding the −226A>G polymorphism were analyzed for potential transcription factor binding sites using TFSEARCH (available at http://www.rwcp.or.jp/papia/). The sequences were similar to the consensus of a caudal-type homeo box (Cdx)-binding site in reverse orientation, and a G for A substitution of the −226A>G polymorphism resulted in disrupting the consensus. Cdx is the family of homeodomain proteins related to the *Drosophila* "caudal" gene, which is required for anterior-posterior regional identity. In the mouse, Cdx1 and Cdx2/3, which are homologs of the *Drosophila* caudal gene, also have functions in anteroposterior patterning and posterior axis elongation (21). In addition, Cdx1 and Cdx2/3 are expressed in the intestine and regulate intestine-specific gene expression (22). The expression of Cdx2/3 is also found in both α- and β-cells (23) and is one of the islet-enriched transcription factors (24). BTC is also predominantly expressed in the endocrine pancreas and intestine (8). This evidence suggests that Cdx protein is a good candidate of the transcription factor, which binds to the region surrounding the −226A>G polymorphism. The −233G>C polymorphism, which is 7 bp upstream from the −226A>G polymorphism, also affected the promoter activity of the *BTC* gene. Because the effects of the −233G>C polymorphism and the −266A>G polymorphisms were not additive, both polymorphisms may affect the binding of an identical transcription factor. The −233G>C polymorphism, however, did not influence the consensus sequence of Cdx binding site on the analysis using TFSEARCH.

It has been recently reported that the Cys7Gly polymorphism in the *BTC* gene is associated with type 2 diabetes in African Americans (25). Our previous study, however, showed that the minor allele frequency was similar between type 2 diabetic patients (1.8%) and nondiabetic subjects (1.8%) in Japanese (15), and the frequency in Japanese patients was lower than in African Americans (32%). Furthermore, no significant difference in the allele frequency between patients and nondiabetic subjects was observed in Caucasians (25). On the other hand, the −226G allele frequency was higher in type 2 diabetic patients than in nondiabetic subjects both in African Americans (25 vs. 20%, $P = 0.14$) and Caucasians (37 vs. 34%, $P = 0.35$) (25), although their differences were not statistically significant. Further studies will be needed to understand the ethnic difference in susceptibility to type 2 diabetes.

ACKNOWLEDGMENTS

This work was supported by a Grant-in-Aid for Scientific Research on Priority Areas "Medical Genome Science" and

by Grant-in-Aid for Scientific Research 13204074 from the Ministry of Education, Culture, Sports, Science and Technology of Japan.

We thank Kanako Fujiuchi for technical assistance.

REFERENCES

1. Butler AE, Janson J, Bonner-Weir S, Ritzel R, Rizza RA, Butler PC: β-Cell deficit and increased β-cell apoptosis in humans with type 2 diabetes. *Diabetes* 52:102–110, 2003
2. Yoon KH, Ko SH, Cho JH, Lee JM, Ahn YB, Song KH, Yoo SJ, Kang MI, Cha BY, Lee KW, Son HY, Kang SK, Kim HS, Lee IK, Bonner-Weir S: Selective beta-cell loss and alpha-cell expansion in patients with type 2 diabetes mellitus in Korea. *J Clin Endocrinol Metab* 88:2300–2308, 2003
3. Sakuraba H, Mizukami H, Yagihashi N, Wada R, Hanyu C, Yagihashi S: Reduced beta-cell mass and expression of oxidative stress-related DNA damage in the islet of Japanese type II diabetic patients. *Diabetologia* 45:85–96, 2002
4. Rhodes CJ: Type 2 diabetes: a matter of beta-cell life and death? *Science* 307:380–384, 2005
5. Nielsen JH, Galsgaard ED, Moldrup A, Friedrichsen BN, Billestrup N, Hansen JA, Lee YC, Carlsson C: Regulation of β-cell mass by hormones and growth factors. *Diabetes* 50 (Suppl. 1):S25–S29, 2001
6. Shing Y, Christofori G, Hanahan D, Ono Y, Sasada R, Igarashi K, Folkman J: Betacellulin: a mitogen from pancreatic beta cell tumors. *Science* 259:1604–1607, 1993
7. Dunbar AJ, Goddard C: Structure-function and biological role of betacellulin. *Int J Biochem Cell Biol* 32:805–815, 2000
8. Seno M, Tada H, Kosaka M, Sasada R, Igarashi K, Shing Y, Folkman J, Ueda M, Yamada H: Human betacellulin, a member of the EGF family dominantly expressed in pancreas and small intestine, is fully active in a monomeric form. *Growth Factors* 13:181–191, 1996
9. Miyagawa J, Hanafusa O, Sasada R, Yamamoto K, Igarashi K, Yamamori K, Seno M, Tada H, Nammo T, Li M, Yamagata K, Nakajima H, Namba M, Kuwajima M, Matsuzawa Y: Immunohistochemical localization of betacellulin, a new member of the EGF family, in normal human pancreas and islet tumor cells. *Endocr J* 46:755–764, 1999
10. Mashima H, Ohnishi H, Wakabayashi K, Mine T, Miyagawa J, Hanafusa T, Seno M, Yamada H, Kojima I: Betacellulin and activin A coordinately convert amylase-secreting pancreatic AR42J cells into insulin-secreting cells. *J Clin Invest* 97:1647–1654, 1996
11. Huotari MA, Palgi J, Otonkoski T: Growth factor-mediated proliferation and differentiation of insulin-producing INS-1 and RINm5F cells: identification of betacellulin as a novel beta-cell mitogen. *Endocrinology* 139: 1494–1499, 1998
12. Yamamoto K, Miyagawa J, Waguri M, Sasada R, Igarashi K, Li M, Nammo T, Moriwaki M, Imagawa A, Yamagata K, Nakajima H, Namba M, Tochino Y, Hanafusa T, Matsuzawa Y: Recombinant human betacellulin promotes the neogenesis of β-cells and ameliorates glucose intolerance in mice with diabetes induced by selective alloxan perfusion. *Diabetes* 49:2021–2027, 2000
13. Li L, Seno M, Yamada H, Kojima I: Betacellulin improves glucose metabolism by promoting conversion of intraislet precursor cells to beta-cells in streptozotocin-treated mice. *Am J Physiol Endocrinol Metab* 285:E577–E583, 2003
14. Saito T, Okada S, Ohshima K, Yamada E, Sato M, Uehara Y, Shimizu H, Pessin JE, Mori M: Differential activation of epidermal growth factor (EGF) receptor downstream signaling pathways by betacellulin and EGF. *Endocrinology* 145:4232–4243, 2004
15. Nakagawa T, Furuta H, Sanke T, Sakagashira S, Shimomura H, Shimajiri Y, Hanabusa T, Nishi M, Sasaki H, Nanjo K: Molecular scanning of the betacellulin gene for mutations in type 2 diabetic patients. *Diabetes Res Clin Pract* 68:188–192, 2005
16. Scheen AJ, Castillo MJ, Lefebvre PJ: Assessment of residual insulin secretion in diabetic patients using the intravenous glucagon stimulatory test: methodological aspects and clinical applications. *Diabetes Metab* 22:397–406, 1996
17. Wacholder S, Chanock S, Garcia-Closas M, El Ghormli L, Rothman N: Assessing the probability that a positive report is false: an approach for molecular epidemiology studies. *J Natl Cancer Inst* 96:434–442, 2004
18. Vague P, Nguyen L: Rationale and methods for the estimation of insulin secretion in a given patient: from research to clinical practice. *Diabetes* 51 (Suppl. 1):S240–S244, 2002
19. Iwasaki Y, Kondo K, Hasegawa H, Oiso Y: C-peptide response to glucagon in type 2 diabetes mellitus: a comparison with oral glucose tolerance test. *Diabetes Res* 25:129–137, 1994
20. Jackson LF, Qiu TH, Sunnarborg SW, Chang A, Zhang C, Patterson C, Lee DC: Defective valvulogenesis in HB-EGF and TACE-null mice is associated with aberrant BMP signaling. *EMBO J* 22:2704–2716, 2003
21. van den Akker E, Forlani S, Chawengsaksophak K, de Graaff W, Beck F, Meyer BI, Deschamps J: Cdx1 and Cdx2 have overlapping functions in anteroposterior patterning and posterior axis elongation. *Development* 129:2181–2193, 2002
22. Walters JR: Cell and molecular biology of the small intestine: new insights into differentiation, growth and repair. *Curr Opin Gastroenterol* 20:70–76, 2004
23. Laser B, Meda P, Constant I, Philippe J: The caudal-related homeodomain protein Cdx-2/3 regulates glucagon gene expression in islet cells. *J Biol Chem* 271:28984–28994, 1996
24. Le Lay J, Matsuoka TA, Henderson E, Stein R: Identification of a novel PDX-1 binding site in the human insulin gene enhancer. *J Biol Chem* 279:22228–22235, 2004
25. Silver K, Tolea M, Wang J, Pollin TI, Yao F, Mitchell BD: The exon 1 Cys7Gly polymorphism within the betacellulin gene is associated with type 2 diabetes in African Americans. *Diabetes* 54:1179–1184, 2005

nature
cell biology

JNK phosphorylation of 14-3-3 proteins regulates nuclear targeting of c-Abl in the apoptotic response to DNA damage

Kiyotsugu Yoshida[1,4], Tomoko Yamaguchi[1], Tohru Natsume[2], Donald Kufe[3] and Yoshio Miki[1,4]

The ubiquitously expressed c-Abl tyrosine kinase localizes to the cytoplasm and nucleus[1,2]. Nuclear c-Abl is activated by diverse genotoxic agents and induces apoptosis[3,4]; however, the mechanisms that are responsible for nuclear targeting of c-Abl remain unclear. Here, we show that cytoplasmic c-Abl is targeted to the nucleus in the DNA damage response. The results show that c-Abl is sequestered into the cytoplasm by binding to 14-3-3 proteins. Phosphorylation of c-Abl on Thr 735 functions as a site for direct binding to 14-3-3 proteins. We also show that, in response to DNA damage, activation of the c-Jun N-terminal kinase (Jnk) induces phosphorylation of 14-3-3 proteins and their release from c-Abl. Together with these results, expression of an unphosphorylated 14-3-3 mutant attenuates DNA-damage-induced nuclear import of c-Abl and apoptosis. These findings indicate that 14-3-3 proteins are pivotal regulators of intracellular c-Abl localization and of the apoptotic response to genotoxic stress.

c-Abl shuttles between the cytoplasm and nucleus by classical mechanisms that involve three nuclear localization signals (NLSs) and one nuclear export signal (NES) in the c-Abl carboxy-terminal region[1,2]. Nuclear c-Abl functions in activating apoptotic signals in the response to DNA damage[3,4]. By contrast, the BCR–ABL fusion protein, which also contains the three NLSs, localizes exclusively in the cytoplasm[5] and confers survival[6]. Forced entrapment of BCR–ABL in the nucleus, however, induces apoptosis[7]. These findings have indicated that the intracellular localization of c-Abl is of importance in dictating whether either survival or apoptosis occurs. The signals that are responsible for targeting c-Abl to the cytoplasm or nucleus are not known.

To investigate partitioning of c-Abl between the cytoplasm and nucleus, we examined subcellular localization of c-Abl before and after genotoxic stress. Treatment of HeLa cells with the DNA-damaging agent adriamycin (ADR), and immunoblot analysis of nuclear and cytoplasmic fractions, showed that c-Abl is targeted to the nucleus (Fig. 1a). As controls, the lysates were reprobed for the nuclear lamin-B and the cytoplasmic IκBα proteins (Fig. 1a). Together with these results, immunostaining of HeLa cells showed nuclear targeting of c-Abl in response to ADR treatment (Fig. 1c). Similar findings were obtained when HeLa cells were treated with other DNA-damaging agents, such as etoposide and ara-C (data not shown). The results also showed that ADR induced nuclear targeting of c-Abl in other cells (see Supplementary Information, Fig. S1a–c). Normal cellular metabolism is associated with the generation of reactive oxygen species (ROS) and c-Abl is activated in the response to oxidative stress[8]. To determine if oxidative stress induces nuclear translocation of c-Abl, cells were treated with hydrogen peroxide as a source of ROS, and nuclear and cytoplasmic lysates were immunoblotted with anti-c-Abl. The results demonstrate that c-Abl is targeted to the nucleus in response to oxidative stress (see Supplementary Information, Fig. S1d). To determine whether nuclear import of c-Abl is transient, cells were analysed during longer periods of ADR exposure. The results indicate that nuclear accumulation of c-Abl is maximal at 2 h and returns to near baseline levels at 8 h (Fig. 1e). In studies with 293T cells expressing Flag-tagged c-Abl (Flag–c-Abl), immunoblot analysis also showed that ADR treatment is associated with localization of c-Abl to the nucleus (Fig. 1b). Immunostaining of the 293T cells confirmed nuclear targeting of Flag–c-Abl in response to ADR (Figs 1d, 3e). Pretreatment with the c-Abl kinase inhibitor, STI571 (ref. 9), had no detectable effect on the ADR-induced nuclear localization of c-Abl (see Supplementary Information, Fig. S1e). Moreover, ADR-induced targeting of a Flag-tagged kinase-inactive c-Abl(K-R)[10] mutant was similar to that of wild-type c-Abl (data not shown), indicating that the c-Abl kinase function is dispensible for nuclear localization. These findings indicate that c-Abl is targeted to the nucleus by a kinase-independent mechanism in the response to DNA damage.

Previous studies have shown that c-Abl-deficient cells are resistant to DNA-damage-induced apoptosis[4] and that activation of nuclear c-Abl is essential for its pro-apoptotic function[10–13]. To determine whether or

[1]Department of Molecular Genetics, Medical Research Institute, Tokyo Medical and Dental University, Tokyo 113-8510, Japan. [2]National Institutes of Advanced Industrial Science and Technology, Biological Information Research Center, 2-41-6 Ohmi, Kohtoh-ku, Tokyo 135-0064, Japan. [3]Dana-Farber Cancer Institute, Harvard Medical School, Boston, MA 02115, USA.
[4]Correspondence should be addressed to K.Y. or Y.M. (e-mail: yos.mgen@mri.tmd.ac.jp or miki.mgen@mri.tmd.ac.jp)

Published online: 6 February 2005, DOI: 10.1038/ncb1228

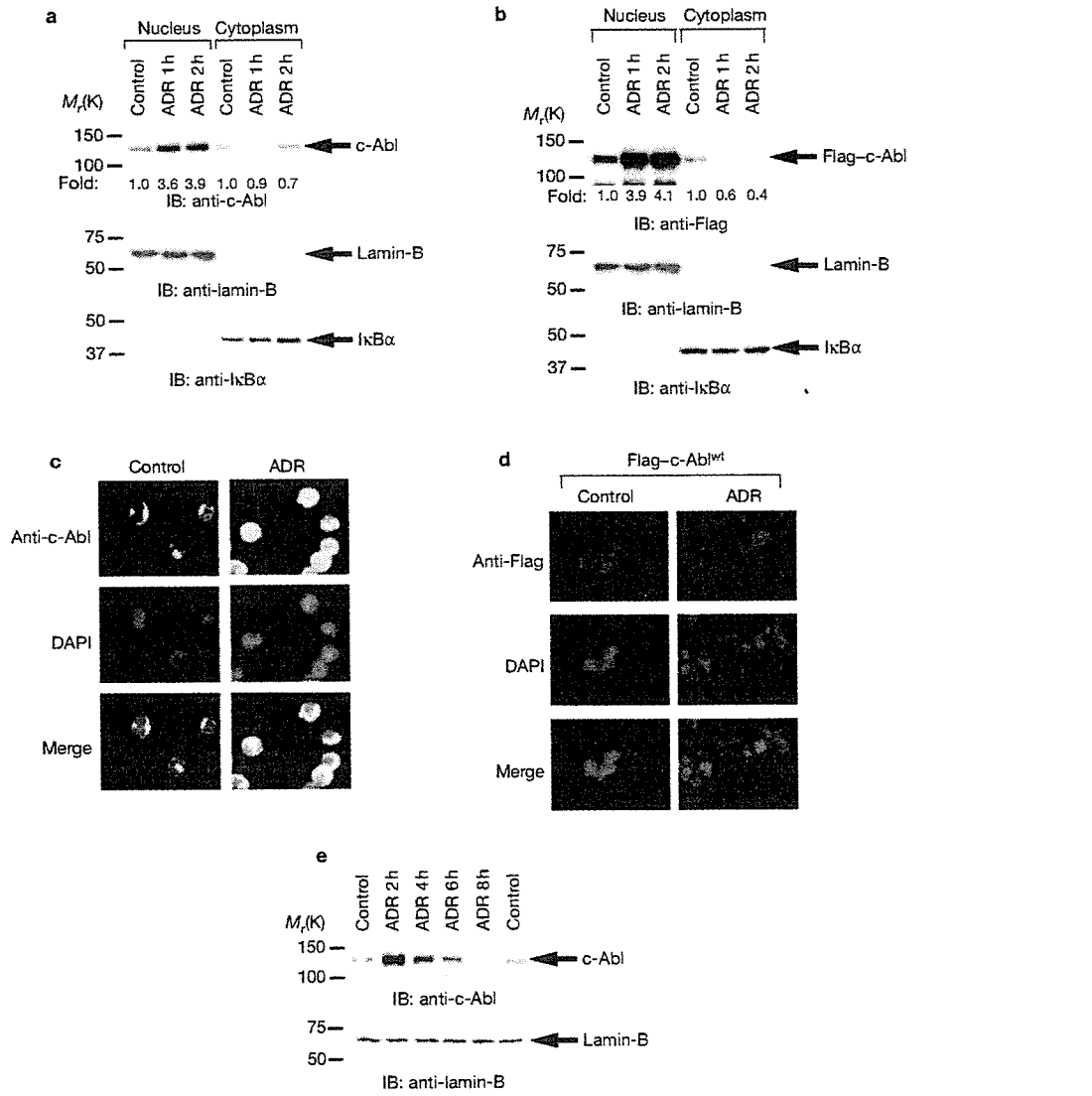

Figure 1 Nuclear translocation of c-ABL in response to DNA damage. (**a**,**b**) HeLa cells (**a**) or 293T cells transfected with Flag–c-ABL (**b**) were left untreated or were treated with adriamycin (ADR). Cell lysates from nuclear and cytoplasmic fractions were subjected to immunoblot (IB) analysis with the indicated antibodies. Protein levels of c-ABL were quantitated by densitometric scanning of the signals. Fold induction was calculated by comparison with the level of nuclear or cytoplasmic c-ABL in control cells. The results are expressed as the mean (standard error, <10%) of at least three independent experiments. (**c**,**d**) HeLa cells (**c**) or 293T cells transfected with Flag-c-ABL (**d**) were left untreated or were treated with ADR for 2 h. After fixation and blocking, cells were incubated with anti- c-ABL (**c**) or anti-Flag (**d**) and counterstained with DAPI (4',6-diamidino-2-phenylindole). Normal mouse immunoglobulin G was used as a negative control (data not shown). (**e**) HeLa cells were treated with ADR for the indicated times. Nuclear lysates were analysed by immunoblotting with anti-c-ABL (upper panel) or anti-lamin-B (lower panel).

not cellular proteins are responsible for subcellular localization of c-Abl, anti-Flag immunoprecipitates from 293T cells expressing Flag–c-Abl were analysed using liquid chromatography, followed by tandem-mass spectrometry[14]. The results indicate that c-Abl associates with 14-3-3 proteins (β, γ, ε, η, σ and ζ). Analysis of anti-14-3-3 immunoprecipitates with anti-c-Abl demonstrated that c-Abl and 14-3-3 proteins form complexes in cells (Fig. 2a). In reciprocal experiments, immunoblot analysis of anti-c-Abl immunoprecipitates with anti-14-3-3 proteins confirmed the association of c-Abl with 14-3-3 proteins (Fig. 2a). When cytoplasmic and nuclear lysates were analysed, the results showed that c-Abl–14-3-3 complexes are localized to the cytoplasm (Fig. 2b). Moreover, treatment with ADR was associated with a marked decrease in these complexes and little, if any, change in localization of 14-3-3 proteins to the cytosol (Fig. 2b,c). Similar results were obtained in response to oxidative stress (see Supplementary Information, Fig. S1d). To determine whether 14-3-3 proteins sequester c-Abl into the cytoplasm, we expressed Flag–c-Abl and green fluorescent protein (GFP) or GFP-14-3-3ζ in 293T cells. Notably, expression of 14-3-3ζ attenuated nuclear localization of c-Abl in control and ADR-treated cells (Fig. 2d). We also knocked-down 14-3-3 proteins by transfection of cells with 14-3-3 small interfering RNAs (siRNAs; Fig. 2e). Downregulation of 14-3-3 proteins was associated with a reduction in cytoplasmic c-Abl